Uranium, rare metals, and granulite-facies metamorphism

Michel Cuney, Pierre Barbey

Geoscience Frontiers 5 (2014) 729–745

Contents lists available at ScienceDirect

China University of Geosciences (Beijing)

Geoscience Frontiers

journal homepage: www.elsevier.com/locate/gsf

Research paper

Uranium, rare metals, and granulite-facies metamorphism

Michel Cuney [a,c,*], Pierre Barbey [b,c]

[a] CNRS, Géoressources, UMR 7359, BP 239, F-54506 Vandœuvre-lès-Nancy, France
[b] CNRS, CRPG, UMR 7358, BP 20, F-54501 Vandœuvre-lès-Nancy Cedex, France
[c] Université de Lorraine, CS 25233, F-54042 Nancy, France

ARTICLE INFO

Article history:
Received 11 September 2013
Received in revised form
13 March 2014
Accepted 20 March 2014
Available online 3 April 2014

Keywords:
Granulite
Carbonic wave
Uranium
Rare metals
Partial melting
Fluorine

ABSTRACT

During granulite-facies metamorphism of metasedimentary rocks by the infiltration of carbonic fluids, the disappearance of hydrated minerals leads to the liberation of aqueous fluids. These fluids are strongly enriched in F and Cl, and a series of Large-Ion-Lithophile (LIL) elements and rare metals, resulting in their depletion in granulites. To sum up the fate of these elements, we focus on three domains representing different crustal levels and showing distinct behaviours with respect to these elements. The Lapland metasedimentary granulites illustrate the behaviour of the LILE and rare metals during lower crustal metamorphism. There is no change in Ba, moderate loss in Rb, and extreme depletion in Cs, Li, and Sn. F and Cl contents are also very low compared to the protoliths or average upper continental crust. Biotite and amphibole breakdown leads to the incorporation of their partitioning into a fluid or a melt.

The Tranomaro metasomatized marbles recrystallizing under granulite-facies conditions represent a demonstrative example of fluid transfer from granulite-facies supracrustals to traps represented by regional scale skarns. Such fluids may be at the origin of the incompatible element enrichment detected in leucosomes of migmatites from St Malo in Brittany (France) and Black Hills in South Dakota. The northern French Massif Central provides us with an example of a potential association between incompatible element enrichment of granitic melts and granulite-facies metamorphism. U- and F-enriched fine-grained granites are emplaced along a crustal scale shear zone active during the emplacement within the St Sylvestre peraluminous leucogranitic complex. We propose that during granulite-facies metamorphism dominated by carbonic waves in a deep segment of the continental crust, these shear zones control: (i) the percolation of F-, LILE-, rare metal-rich fluids liberated primarily by the breakdown of biotite; (ii) the enhancement of partial melting by F-rich fluids at intermediate crustal levels with the generation of F-, LILE-, rare metal-rich granitic melts; (iii) their transfer through the crust with protracted fractionation facilitated by their low viscosity due to high F-Li contents; and finally (iv) their emplacement as rare metal intrusions at shallow crust levels.

1. Introduction

Granulite-facies rocks are a fundamental component of the continental crust, which encompass (1) dominantly mafic cumulates and gabbros in the lowermost crust, resulting from underplating by mantle magmas; they are mostly known from xenoliths in basalts; and (2) high-grade supracrustal rocks buried in the lower crust during orogenic processes. Regardless of their origin, they share three main characteristics: (1) they correspond to rocks (almost) free of OH-bearing silicates (micas and amphiboles); (2) they contain high-density, CO_2-rich, fluid inclusions; and (3) they are generally poor or depleted in large ion lithophile (LIL) elements. These three basic features led to two distinct models for the generation of granulite-facies rocks.

The first model relies on the pioneering work of J. Touret (1970, 1971) which showed that granulites are characterized by the presence of carbonic fluid inclusions. This, together with the observation of incipient charnockitization (Pichamuthu, 1960;

* Corresponding author. CNRS, Géoressources, UMR 7359, BP 239, F-54506 Vandœuvre-lès-Nancy, France.
E-mail address: michel.cuney@univ-lorraine.fr (M. Cuney).

Peer-review under responsibility of China University of Geosciences (Beijing)

Production and hosting by Elsevier

1674-9871/$ – see front matter © 2014, China University of Geosciences (Beijing) and Peking University. Production and hosting by Elsevier B.V. All rights reserved.
http://dx.doi.org/10.1016/j.gsf.2014.03.011

Table 1
Trace element concentrations in Lapland granulites. Data from Hörmann et al. (1980) and Raith et al. (1982) for samples with the code letter R, and from Barbey and Cuney (1982) and this study (*) for samples with the code letter L.

(ppm)	K	Ba	Rb	Sr	Cs	Li	Sn	F(*)	Cl(*)	K/Rb	K/Ba	Rb/Sr	Rb/Cs	La/Th	Th/U	K/Th	K/U
Sillimanite-garnet gneiss																	
L176	35,184		91	279		5	0.1			387		0.33			14.5	3466	50,262
L188	31,200	949	113	156	0.69	7.7	0.1	760	117	276	32.9	0.72	164	4.6	13.7	3257	44,572
L313	21,824	918	82	167	0.50	9.5	0.7	610	76	266	23.8	0.49	164	2.9	13.7	1141	15,588
L371	28,960	1155	101	229	0.23	6	0.1	140	102	287	25.1	0.44	439	4.6	22.4	3236	72,400
L389	39,498	1201	136	255	0.29	4.8	0.25	150	170	290	32.9	0.53	469	3.1	12.2	2310	28,213
L530	27,632		111	176		8	0.1			249		0.63			32.9	1400	46,054
L555	29,707	843	101	171	0.49	4.8	0.4	170	111	294	35.2	0.59	206	3.0	23.0	1618	37,134
L558	27,217	1062	116	187	0.39	6	0.12	480	149	235	25.6	0.62	297	3.3	16.2	1523	24,743
L581	27,632	831	79	185	0.25	4.2	0.1	30	152	350	33.3	0.43	316	5.9	11.5	4010	46,054
L599	19,915	962	109	194	0.48	7.4	0.1	360	173	183	20.7	0.56	227	3.3	7.7	1298	9958
L959	30,537	867	118	147	0.36	6.5	0.2	740	71	259	35.2	0.80	328	3.3	34.4	1773	61,073
L963	37,507	1248	102	274	0.22	6.9	0.5	330	139	368	30.1	0.37	464	4.1	48.1	2597	125,023
R57II	16,845	632	65			20				259	26.7						
R59I	29,790	932	107	125		4				278	32.0	0.86					
R94I	22,571	1373	102	371		15				221	16.4	0.27					
Garnet gneiss																	
L308	26,886	1307	87	291	0.15	3.8	0.1	20	102	309	20.6	0.30	580	7.4	15.3	5870	89,618
L315	28,213		54	224		4.3	0.25			522		0.24			15.5	2273	35,267
L316	19,334	609	68	157	0.20	4.9	0.7	390	133	284	31.7	0.43	340	3.8	20.7	1868	38,669
L319	4647	195	16	135	0.18	4.6	0.75	270	112	290	23.8	0.12	89	17.4	2.8	4076	11,334
L360	25,392	1396	55	200	0.11	2.6	0.15	40	116	462	18.2	0.28	500	4.8	9.5	4439	42,320
L375	29,458	1025	85	209	0.13	4.6	0.4	330	141	347	28.7	0.41	654	6.5	68.4	4307	294,579
L515	26,139	845	98	343	0.27	12.5	0.15	650	118	267	30.9	0.29	363	4.3	15.3	3412	52,277
L516	28,628	874	106	154	0.19	8.4	0.1	270	99	270	32.8	0.69	558	4.7	12.5	3822	47,714
L517	15,102	513	41	336	0.12	5.6	0.1	20	124	368	29.4	0.12	342	13.4	16.3	4633	75,512
L523	32,279	1380	75	566	0.28	6.9	1	140	317	430	23.4	0.13	268	4.1	52.6	2044	107,597
L526	21,326	761	80	136	0.12	4.2	0.15	70	120	267	28.0	0.59	667	3.4	13.6	1957	26,657
L527	23,566	782	80	178	0.11	4.5	0.25	150		295	30.1	0.45	727	3.7	18.8	2512	47,133
L565	12,198	652	38	264	0.13	3.3	0.1	490	635	321	18.7	0.14	292	3.9	21.3	638	13,553
L580	13,941	723	83	336	0.59	11	2.3	130	136	168	19.3	0.25	141	3.0	26.2	591	15,490
L601	12,779	598	52	174	0.26	4	0.1	490	348	246	21.4	0.30	200	3.4	14.1	1135	15,974
L602	37,673	1003	80	289	0.28	4	0.1	300	720	471	37.6	0.28	286	3.7	27.4	2290	62,788
L604	18,339	537	51	199	0.11	2.8	0.1	70	124	360		0.26	464	3.3	17.2	1523	26,198
L684	13,111	443	55	335	0.54	10.2	0.3	950	240	238	29.6	0.16	102	3.9	9.0	1318	11,919
L838	27,798	818	88	163	0.19	3.3	0.12	20	140	316	34.0	0.54	463	8.0	11.1	6275	69,496
L969	27,134	958	83	216	0.15	7.8	0.6	30	73	327	28.3	0.38	553	3.2	49.1	1842	90,448
R57III	16,264	796	55	297		12				296	20.4	0.19					
R58II	9543	415	32	607		13				298	23.0	0.05					
R61I	11,451	260	23	27		2				498	44.0	0.85					
R69I	11,617	1399	51	353		13				228	8.3	0.14					
R70II	14,107	486	51	153		3				277	29.0	0.33					
R86I	7302	291	53	267		7				138	25.1	0.20					
R96I	12,862	398	35	366		5				367	32.3	0.10					
R102I	13,360	447	72	276		11				186	29.9	0.26					
R109II	9045	327	26	311		9				348		0.08					
R111I	7966	811	32	182		10				249	9.8	0.18					
R128I	10,373	496	49	272		10				212	20.9	0.18					
R150I	26,139	878	71	166		4				368	29.8	0.43					
RJ10II	8630	416	49	475		11				176	20.7	0.10					
RJ3I	2821	112	12	138		4				235	25.2	0.09					
RJ5II	10,787	337	40	119		4				270	32.0	0.34					
RJ7I	15,683	545	89	238		7				176	28.8	0.37					
Light garnet-alkali-feldspar gneiss																	
L370	32,030	1170	77	320	0.17	2.5	0.1	<20	170	416	27.4	0.24	453	12.5	10.0	16,015	160,151
L528	38,503	809	103	198	0.15	2.7	0.25	<20	178	374	47.6	0.52	687	1.7	10.0	9626	96,257
L529	43,150		123	270		3.5	0.32			351		0.46			10.0	21,575	215,748
L557	49,456	1404	128	226	0.15	5	0.12	50	139	386	35.2	0.57	853	4.5	16.1	5114	82,427
L862	37,922	332	65	94	0.04	1	0.25	<20	144	583	114.2	0.69	1625	2.0	8.2	9295	75,844
R76I	55,016		149	267		4				369		0.56					
R116I	30,205	1229	71	171		4				425	24.6	0.42					
R130I	33,026		46	50		2				718		0.92					
R143I	61,986	877	125	137		6				496	70.7	0.91					
R148I	43,730	1416	148	273		7				295	30.9	0.54					
R154I	24,894	540	39	95		6				638	46.1	0.41					
R156I	22,073	554	77	198		6				287	39.8	0.39					
Garnet-quartz gneiss																	
L567	12,447	509	40	145	0.11	3.5	0.1	490	80	311	24.5	0.28	364	3.6	13.4	1548	20,745
L577	5477	252	6	255	0.05	6	0.1	60	66	913	21.7	0.02	120	3.4	14.5	629	9128
L690	9128		35	79		3.1	0.2			261		0.44			13.8	367	5071
R69II	2738	147	9	77		4				304	18.6	0.12					
Calc-silicate rock																	
L583	913	42	5	188	0.20	2	2.4	180	825	183	21.7	0.03	25	2.2	3.2	93	299

Table 1 (*continued*)

(ppm)	K	Ba	Rb	Sr	Cs	Li	Sn	F(*)	Cl(*)	K/Rb	K/Ba	Rb/Sr	Rb/Cs	La/Th	Th/U	K/Th	K/U
L1611	8049	501	31	156	0.15	12.7	2.5	220	2330	260	16.1	0.20	207	2.2	3.9	724	2834
R101I	7468	352	42	173		4				178	21.2	0.24					

ppm	Th	U	Zr	La	Ce	Pr	Nd	Sm	Eu	Gd	Tb	Dy	Ho	Er	Tm	Yb	Lu
Sillimanite-garnet gneiss																	
L176	10.15	0.7															
L188	9.58	0.7	206	44.2	84.29	18.00	32.79	6.14	1.51	6.00	1.00	5.79	1.20	2.93	0.47	3.00	0.48
L313	19.13	1.4	213	55.2	109.40	11.77	44.22	7.46	1.41	5.50	0.83	5.09	1.13	2.82	0.49	3.29	0.49
L371	8.95	0.4	228	40.9	67.39	6.43	22.91	4.33	1.85	4.83	0.75	4.62	1.06	2.69	0.44	2.88	0.47
L389	17.10	1.4	182	53.7	102.40	11.55	41.76	7.20	1.97	5.90	0.93	5.36	1.22	3.23	0.51	3.38	0.51
L530	19.74	0.6	229														
L555	18.36	0.8	172	54.7	104.40	11.77	44.04	7.77	1.42	6.85	1.14	7.16	1.65	4.50	0.74	4.68	0.67
L558	17.87	1.1	284	59.0	109.30	11.74	42.24	7.34	2.04	6.24	0.91	5.00	1.08	2.78	0.43	2.76	0.46
L581	6.89	0.6		40.9	74.21	7.40	27.08	4.45	1.71	4.53	0.92	6.76	1.62	4.51	0.78	5.22	0.77
L599	15.34	2.0	183	50.9	98.90	11.04	38.85	6.82	1.68	5.90	0.84	4.72	1.09	2.96	0.46	2.90	0.46
L959	17.22	0.5	180	56.6	104.30	11.25	43.65	7.87	1.70	7.00	1.20	7.22	1.63	4.37	0.67	4.43	0.76
L963	14.44	0.3	235	58.7	110.40	11.42	42.18	6.87	1.76	6.45	0.95	5.79	1.27	3.37	0.53	3.49	0.56
Garnet gneiss																	
L308	4.58	0.3	224	34.0	52.92	5.04	17.29	3.22	1.92	3.98	0.75	4.61	0.99	2.51	0.39	2.50	0.39
L315	12.41	0.8															
L316	10.35	0.5	181	39.2	79.48	8.31	31.48	5.57	1.24	5.00	0.72	4.45	0.97	2.38	0.35	2.24	0.37
L319	1.14	0.41	235	19.8	34.13	3.28	11.25	2.00	0.80	3.04	0.67	4.58	1.18	3.27	0.52	3.47	0.56
L360	5.72	0.6	276	27.4	46.87	4.48	16.16	2.77	1.83	2.86	0.55	3.83	0.87	2.16	0.35	2.40	0.41
L375	6.84	0.1	200	44.2	77.38	7.75	26.62	4.22	1.53	4.13	0.64	3.76	0.83	2.06	0.32	2.16	0.33
L515	7.66	0.5	102	32.8	65.20	6.67	23.56	3.50	2.00	2.76	0.36	1.95	0.39	1.02	0.16	1.02	0.17
L516	7.49	0.6	242	35.4	68.03	7.00	25.45	4.81	1.24	4.65	0.71	3.76	0.79	2.14	0.34	2.13	0.34
L517	3.26	0.2	119	43.8	92.93	10.08	36.00	5.17	1.87	4.23	0.56	3.56	0.84	2.23	0.36	2.41	0.39
L523	15.79	0.3	161	64.9	115.80	12.16	41.20	5.57	2.19	4.33	0.60	3.70	0.85	2.28	0.35	2.27	0.34
L526	10.90	0.8	231	37.2	71.72	7.54	28.59	5.26	1.18	4.78	0.73	4.40	0.91	2.32	0.35	2.19	0.34
L527	9.38	0.5	220	34.6	67.83	6.78	24.75	4.31	1.22	3.98	0.64	3.81	0.85	2.32	0.36	2.46	0.37
L565	19.13	0.9	226	74.5	146.40	17.08	61.59	9.24	1.87	8.04	1.16	6.25	1.25	3.10	0.49	2.99	0.48
L580	23.60	0.9	274	69.7	138.50	16.28	62.12	10.57	1.77	8.24	1.12	5.58	1.16	3.07	0.45	2.92	0.47
L601	11.26	0.8	223	38.4	74.11	7.71	29.92	4.78	1.24	3.83	0.56	3.12	0.69	1.94	0.33	2.31	0.39
L602	16.45	0.6	229	60.1	115.60	12.54	46.60	6.65	2.27	4.40	0.51	2.48	0.48	1.27	0.18	1.20	0.20
L604	12.04	0.7	300	39.3	76.28	8.32	30.25	5.45	1.27	4.74	0.74	4.05	0.93	2.56	0.43	2.79	0.43
L684	9.95	1.1	189	39.1	80.55	8.97	34.30	6.40	1.47	5.09	0.77	4.21	0.82	2.06	0.31	1.89	0.28
L838	4.43	0.4	184	35.5	58.73	5.93	20.61	3.93	1.47	3.84	0.62	3.70	0.88	2.18	0.33	2.12	0.36
L969	14.73	0.3	233	47.1	90.45	9.47	35.74	6.12	1.37	4.91	0.74	4.23	0.84	2.21	0.33	2.21	0.33
Light garnet alkali-feldspar gneiss																	
L370	2.00	0.2	73	25.1	43.27	4.41	14.40	1.98	2.17	1.74	0.28	1.76	0.47	1.36	0.24	1.55	0.22
L528	4.00	0.4	34	6.8	12.22	1.20	3.74	0.55	1.15	0.57	0.12	1.02	0.31	1.11	0.25	1.96	0.34
L529	2.00	0.2															
L557	9.67	0.6	156	43.5	74.01	7.39	26.60	3.64	2.14	3.12	0.49	2.52	0.47	1.12	0.16	1.02	0.17
L862	4.08	0.5	42	8.3	13.04	1.22	3.51	0.40	0.54	0.34	0.05	0.56	0.16	0.58	0.15	1.24	0.18
Garnet-quartz gneiss																	
L567	8.04	0.6	287	29.1	59.81	5.92	21.43	3.33	0.82	2.88	0.33	1.42	0.24	0.52	0.08	0.54	0.10
L577	8.71	0.6	201	29.4	58.70	6.13	23.34	4.02	0.95	3.55	0.54	3.09	0.65	1.75	0.29	1.86	0.31
L690	24.88	1.8	427														
Calc-silicate rocks																	
L583	9.86	3.05	166	21.6	50.6	5.5	21.5	4.2	0.8	3.5	0.5	2.8	0.6	1.4	0.2	1.5	0.2
L1611	11.11	2.84	204	24.3	55.3	5.8	22.4	4.2	0.9	3.5	0.6	3.7	0.8	2.1	0.4	2.1	0.3

Analytical methods: (1) sample code letter L: K determined by X-ray fluorescence spectrometry (Govindaraju and Montanari, 1978); Rb and Sr by X-ray fluorescence spectrometry (Jahn et al., 1980); Ba, Cs and Sn by atomic emission spectrometry (Govindaraju and Mevelle, 1987); F and Cl determined by potentiometry and by spectrophotometry (Vernet et al., 1987); U, Th and the rare-earth elements were determined at CRPG (CNRS, Nancy) respectively by fluorimetry, γ-spectrometry and atomic emission spectrometry using an inductively coupled plasma source (Govindaraju and Mevelle, 1987). (2) Sample code letter R: K, Rb, Sr, Ba and Li determined by atomic absorption spectrometry (Maxwell, 1968).

Janardhan et al., 1982; Hansen et al., 1987; Raith et al., 1990), led him, and some years later Newton et al. (1980), to propose the concept of "carbonic metamorphism". In this model, granulites are interpreted to result from the passage of a CO_2 wave, which flushes out water leading to the formation of dehydrated granulites at the base of the continental crust. In this model, micas and amphiboles break down under subsolidus conditions due to a series of dehydration reactions (cf. Touret and Hartel, 1990). The additional role of high salinity aqueous fluids has been later emphasized in destabilizing OH-bearing mineral phases, and as a significant agent in wide metasomatic processes (see the recent papers by Touret and Huizenga, 2011; Touret and Nijland, 2013).

The second model is based on the depletion of granulites in LIL by partial melting (e.g. Heier, 1973; Collerson, 1975; Gray, 1977; Dostal and Capedri, 1978). This model also appeared in the literature in the early seventies (Brown and Fyfe, 1970; Fyfe, 1973) and was subsequently the subject of several experimental and theoretical approaches (Thompson, 1982; Clemens and Vielzeuf, 1987; Le Breton and Thompson, 1988; Vielzeuf and Holloway, 1988; Clemens, 1990; among others). In this model known generally as "fluid-absent melting" or "dehydration melting", OH-bearing mineral phases destabilize through incongruent melting to produce water-undersaturated granitic melts and residual dehydrated crystalline assemblages (granulites). Melts are extracted from the melting zone giving rise to granitic bodies in the upper crust and preventing back reactions on cooling (e.g. Kriegsman and Hensen, 1998; Kriegsman, 2001). Granulites are then viewed as restites and the whole melting process leads to a differentiated "sterile" lower crust (Vielzeuf et al., 1990).

Beyond the processes involved in the generation of granulite-facies rocks (anyway rather complementary than opposed, since granulite-facies metamorphism is not restricted to a unique fluid regime), the most fundamental aspect of granulite-facies metamorphism is the breakdown of micas and amphiboles, releasing large amounts of incompatible elements (Cl, F, Li, Rb, Sn, Ta, W, U, etc.), which may have significant compositional effects on the magmas generated in mid-crustal domains above granulitized domains. Contrary to models proposing LILE depletion in granulites, it should be noted that granulites enriched in radioactive elements have been reported in the western Namaqualand (Andreoli et al., 2006) and in the Limpopo Belt, South Africa (Andreoli et al., 2011). The origins behind this enrichment will be speculated on below.

The principal objective of this paper is to present new geochemical data attesting to the depletion of the Lapland metasedimentary granulites with a large set of incompatible elements and to discuss the status of the elements removed during granulite-facies metamorphism by dehydration processes, such as infiltration by CO_2-rich fluids or dehydration melting. A second objective is to discuss how and where these elements are transferred. This includes either their collection into partial melts within geological units, which play the role of traps leading to possible mineral concentrations, or their dispersion into overlying geological units.

2. Depletion in large ion lithophile (LIL) elements

We present here an example of the contrasting behaviour between trace elements (including Li, Cs, Sn, F, Cl) during granulite-facies metamorphism, utilizing the granulites of Lapland as a case study. These granulites have been interpreted as a pile of metasediments thrusted onto the South Lapland craton during the Palaeoproterozoic (e.g. Meriläinen, 1976; Barbey et al., 1984; Barbey and Raith, 1990; Marker et al., 1990; Daly et al., 2001; Tuisku and Huhma, 2006; Cagnard et al., 2011). Burial of the sediments was accompanied by localized thrusts during regional-scale horizontal shortening associated with prograde medium-pressure metamorphism (800–850 °C and 0.7–0.8 GPa). The whole evolution, from deposition and burial of the sediments to exhumation, lasted between 1.94 and 1.87 Ga. The Lapland Granulite Belt has been subdivided, on the basis of strain intensity and seismic data, into sheared granulites in its western and southern parts (basal unit) and cordierite-bearing diatexites mainly located in its eastern upper part (Meriläinen, 1976; Hörmann et al., 1980; Gaál et al., 1989; Elo, 2006).

The Lapland granulites consist dominantly of garnet-sillimanite gneisses (metashales), garnet gneisses (metagreywackes), garnet-alkali-feldspar gneisses (felsic metavolcanites), and minor quartz-rich garnet gneisses (metasandstones) and calc-silicates rocks (calcareous metasiltstones). They are associated with norites and enderbites interpreted as metaplutonic rocks (Barbey and Raith, 1990). A study of the concentrations of a limited suite of trace elements in the Lapland granulites (Barbey and Cuney, 1982) showed that LIL are controlled, with variable degrees of depletion, among several factors by the nature of the protoliths and the mineralogy of the granulites. Similar observations were made by Rudnick and Presper (1990) from a larger sampling of both granulite terrains and lower crustal xenoliths. These last authors distinguished between granulites with $K > 1$ wt.% showing high K/U and K/Cs but low to moderate K/Rb ratios, and granulites with $K < 0.5$ wt.% showing high K/U, K/Cs, and K/Rb ratios. We discuss here the behaviour of LIL in the Lapland granulites, which were dominantly derived from sedimentary or volcano-sedimentary protoliths (Hörmann et al., 1980; Barbey et al., 1982; Barbey and Cuney, 1982; Raith et al., 1982), to which is added new Li, Sn, F, Cl and REE data (Table 1).

2.1. K, Rb, Sr, Cs and Ba

Average Rb contents and K/Rb ratios vary as a function of rock type, and are in the same compositional range as other granulite-facies terrains and xenoliths worldwide (Fig. 1a). In sillimanite garnet gneisses, the average Rb content (102 ± 18 ppm; range 65–136 ppm) and K/Rb ratio (280 ± 54; range 183–387) differ from the values given by the post-Archaean average Australian shale (Taylor and McLennan, 1985), which gives higher Rb contents (160 ppm) and lower K/Rb ratios (192). The sillimanite garnet gneiss Rb content, however, is close to the average upper crustal value (Rb = 112 ppm, K/Rb = 252). The K/Rb ratios show a slightly positive correlation with the K contents (Fig. 1a). In garnet gneisses, the average Rb content (59 ± 24 ppm, range 16–106 ppm) and K/Rb

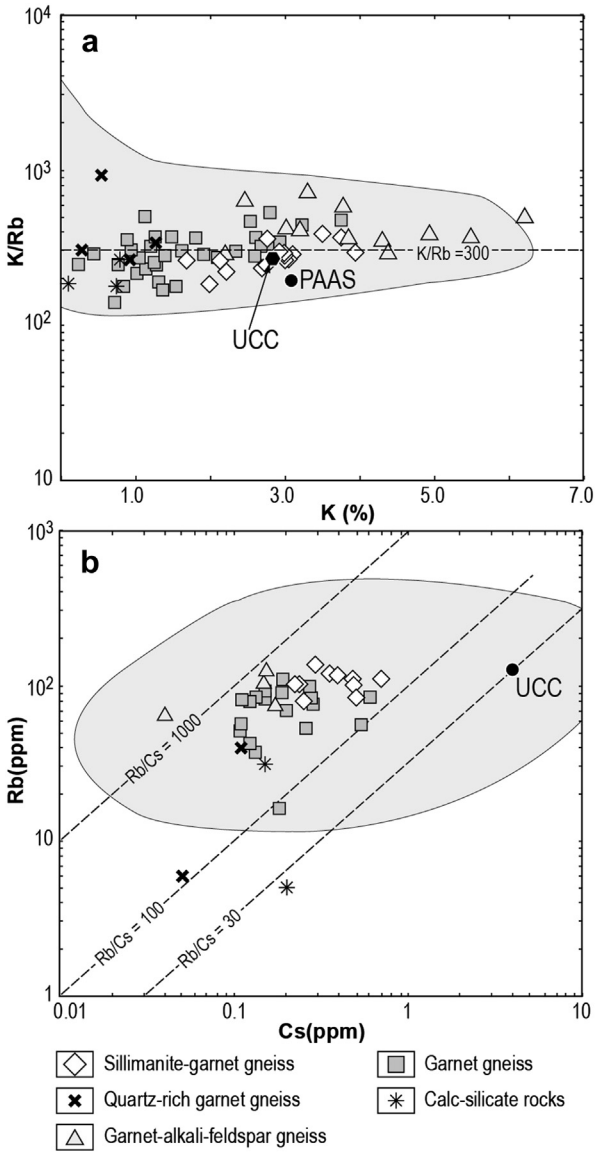

Figure 1. Plots of K/Rb vs. K (a) and Rb vs. Cs (b) for the Lapland granulites. PAAS = Post-Archaean Average Australian Shales; UCC = Average Upper Continental Crust (Taylor and McLennan, 1985). Gray shaded fields: Granulite-facies Archaean and post-Archaean terrains from Rudnick and Presper (1990).

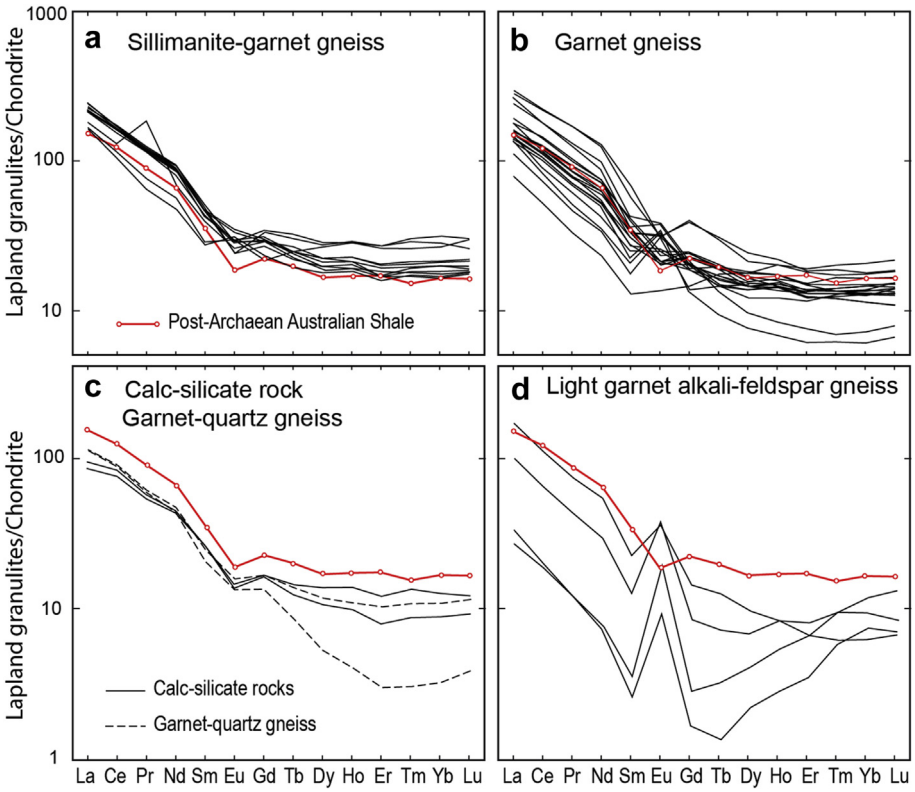

Figure 2. Rare-earth element patterns normalized to chondrite (Evensen et al., 1978) for the Lapland granulites. Post-Archaean average Australian shales from Taylor and McLennan (1985).

ratio (302 ± 93, range 138–522) are, respectively, lower and higher than values recorded in Phanerozoic greywackes, e.g. K/Rb ratios range from 150 to 300 (Senior and Leake, 1978; Taylor and McLennan, 1985), though there is a significant overlap. Here again, the K/Rb ratios are slightly correlated with K contents. In garnet-alkali-feldspar gneisses, the average Rb content is 96 ± 38 ppm (range 39–149 ppm), and the average K/Rb ratio is high (445 ± 137; range 287–718). Note that in all these rock types the samples with the lowest K/Rb ratios (<200) contain significant amounts of biotite. Quartz-rich garnet gneisses and calc-silicate rocks have low Rb contents, around 25 ppm on average, with variable but relatively high K/Rb ratios (178–304, with one value up to 913). As outlined by Barbey and Cuney (1982), the range in Sr concentrations (94–371 ppm, with the exception of few outlying values) remains within those of equivalent sedimentary rock types (e.g. Veizer, 1978). For the majority of the samples (75%) Rb/Sr ratios (average 0.37 ± 0.22) are higher than 0.20. Additionally, $^{87}Sr/^{86}Sr$ initial ratios of around 0.705 are typical of crustal material and consistent with the assumed source of the sediments (Bernard-Griffiths et al., 1984). As a whole, the Rb contents and K/Rb ratios in the Lapland metasedimentary granulites remain close to the crustal average, showing only limited depletion in Rb.

Concentrations in Cs are very low, lower than 1 ppm (Fig. 1b). However, they are higher in metashales (0.39 ± 0.15 ppm, range 0.22–0.69) than in metagreywackes (0.22 ± 0.14, range 0.11–0.59 ppm) or garnet-alkali-feldspar gneisses (0.13 ± 0.06, range 0.04–0.17 ppm). These values are well within the range of composition given for post-Archaean granulite terrains (0.01 < Cs < 10 ppm; Rudnick and Presper, 1990). Therefore, despite their low Rb contents, the Lapland granulites have very high Rb/Cs ratios (>300) compared to the average upper continental crust (Rb/Cs = 30). Only quartz-rich garnet gneisses and calc-silicate rocks show lower Rb/Cs ratios (25–364), but the corresponding Cs contents remain very low (0.05–0.20 ppm).

Lastly, the Ba contents do not show any evidence of concentration variation related to metamorphism, with respect to equivalent sedimentary rocks (Barbey and Cuney, 1982). K/Ba ratios are quite similar in sillimanite garnet gneisses and garnet gneisses (27 ± 7 ppm, range 8–44), though the range in Ba content is more variable in garnet gneisses (Table 1). Quartz-rich garnet gneisses and calc-silicate rocks show slightly lower K/Ba ratios (21 ± 3), whereas garnet-alkali-feldspar gneisses have higher and more variable ratios (48 ± 28, range 25–114). These values are comparable to those of the Archaean and post-Archaean granulite-facies terranes (K/Ba = 26 and 34, respectively) and not significantly different from K/Ba ratios in sedimentary siliciclastic rocks (30 to 61 in shales and greywackes; van de Kamp et al., 1976; Senior and Leake, 1978; Taylor and McLennan, 1985).

In conclusion, the behaviour of Ba, Rb and Cs during granulite-facies metamorphism is highly contrasting, with no evidence of change in Ba content, moderate loss in Rb and extreme depletion in Cs with respect to K. These differences are related to the breakdown of biotite, with K-feldspar becoming the major mineral phase controlling these elements under granulite-facies conditions. The behaviour of these elements is thus dependent on their larger incorporation relative to K in the lattice of biotite with respect to K-feldspar and, thus, on mineral/fluid or mineral/melt partitioning. Experimental studies on Rb, Cs, Sr and Ba fractionation between feldspars, silicate melts, and solutions (e.g. Carron and Lagache, 1980) and measurements of partition coefficients between biotite, feldspars and silicic melts (e.g. Nash and Crecraft, 1985) show that Ba and Sr enter the crystalline phase, whereas Rb and especially Cs appear incompatible and are thus released in the fluid phase or the melt phase.

2.2. REE, Th, U

Sillimanite-garnet gneisses and garnet gneisses show REE patterns closely similar to that of post-Archaean Australian shales (PAAS), with average normalized $[La/Yb]_N$ and Eu/Eu* ratios of 9.6 and 0.8 compared to 9.2 and 0.7 for PAAS, respectively (Fig. 2a, b). The patterns of quartz-rich garnet gneisses and calc-silicate rocks do not show significant differences with those of equivalent sedimentary protoliths (Fig. 2c). Therefore, there is no evidence of discernible changes in REE concentrations in association with granulite-facies metamorphism.

Th and U show distinct behaviour in the Lapland granulites. Th concentrations decrease from sillimanite-garnet gneisses (14.6 ± 4.5 ppm) to garnet gneisses (10.4 ± 5.6 ppm) and garnet-alkali-feldspar gneisses (4.4 ± 3.1 ppm), and are in the range of common post-Archaean sediments. Calc-silicate rocks and quartz-rich garnet gneisses show concentrations around 10 ppm, with the exception of one value at 24.9 ppm. Th is closely correlated to La (Fig. 3a) and to the total REE content, with La/Th ratios within the range of sedimentary rocks; this indicates no significant La/Th fractionation during granulite-facies metamorphism and a control by accessory phases (mostly monazite and xenotime). Uranium concentrations range from 0.1 to 3.05 ppm but are mostly <1 ppm, with the exception of the calc-silicate rocks where U contents are around 3 ppm and some graphite-rich metapelites where the U content reaches 16 ppm (Barbey and Cuney, 1982). Th/U ratios are variable. They are very high in metapelites and metagreywackes (21), in garnet-alkali-feldspar gneisses and quartz-rich garnet gneisses (12), and close to the average upper crustal value (3.8; Taylor and McLennan, 1985) in the calc-silicate rock samples (3.6). Th/U ratios are almost independent from the La/Th ratio (Fig. 3b), therefore suggesting loss in U for most lithologies. The only exceptions are calc-silicate rocks, which show low Th/U ratios and graphite-rich metapelites with very low Th/U ratios indicating no depletion in U. In the calc-silicate rocks, titanite which is the main phase hosting U, as shown by α-track distribution (Barbey and Cuney, 1982), remains stable during high-grade metamorphism, and thus prevents U leaching from this type of lithology. In the metapelites, the presence of graphite imposes low redox conditions and consequently very low U solubility in the fluids, explaining why U is not depleted from such rocks.

2.3. Li, Sn, F and Cl

Li contents are in the same range in all rock types (1 to 13 ppm), with the exception of two higher values at 15 and 20 ppm in garnet gneisses. Average contents are 7.7 ± 4.4 ppm in sillimanite-garnet gneisses, 6.6 ± 3.4 ppm in garnet gneisses, 4.1 ± 1.9 ppm in garnet-alkali-feldspar gneisses, 4.2 ± 1.3 ppm in quartz-rich garnet gneisses and 6.2 ± 5.7 ppm in calc-silicate rocks. These concentrations are comparable to those given for granulite-facies post-Archaean terrains and xenoliths (around 6–7 ppm on average; Rudnick and Presper, 1990), but lower than the average upper continental crust (20 ppm). More significantly, the Li values recorded in the granulites of Lapland are lower by almost one order of magnitude compared to those of equivalent sedimentary rocks (e.g. 60–75 ppm in average post-Archaean shales; Taylor and McLennan, 1985).

Tin also shows very low concentrations (≤0.7 ppm) in most types of Lapland granulites, with the notable exception of calc-silicate rocks containing on average 2.5 ppm Sn. These values are very low compared to the 5.5 ppm content retained for the average upper continental crust, and are also lower than those reported for granulite-facies terrains (2.7 ppm) and xenoliths (1.6 ppm) (Rudnick and Presper, 1990). More particularly, the sillimanite

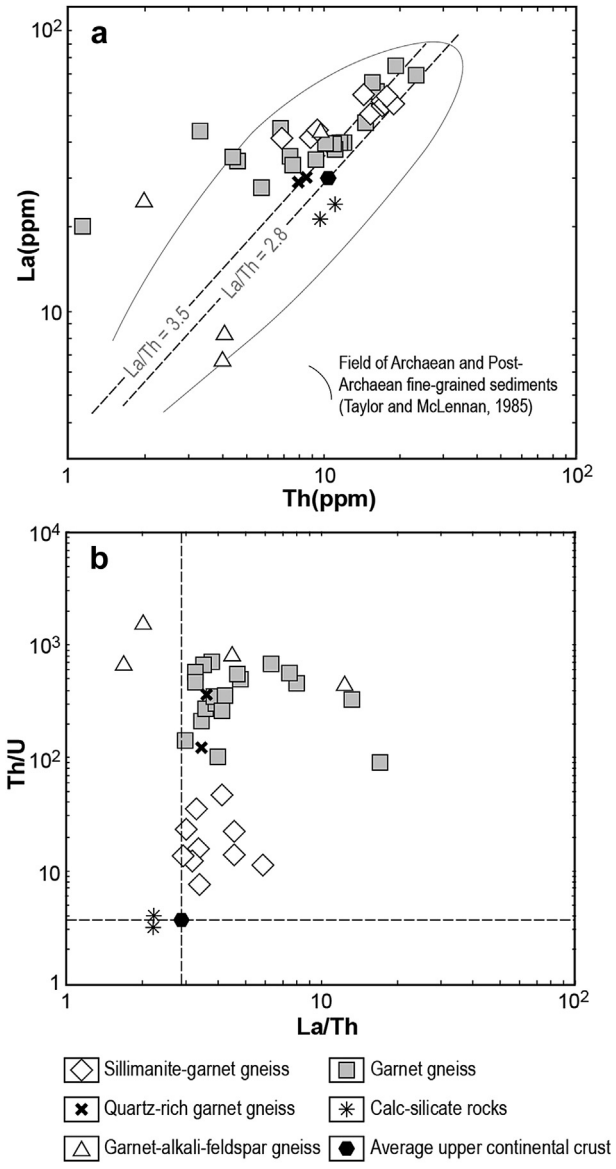

Figure 3. Plots of La vs. Th (a) and Th/U vs. La/Th (b) for the Lapland granulites. Average La/Th ratios for Archaean (3.5) and post-Archaean (2.8) sediments, and average upper continental crust from Taylor and McLennan (1985).

garnet gneisses have extremely low Sn contents (average: 0.2 ± 0.2 ppm) with respect to average post-Archaean shales showing contents >4 ppm (Taylor and McLennan, 1985).

Fluorine and Cl contents are also low in the Lapland granulites. Fluorine contents (average 282 ppm) are in the same range in all rock types (20–950 ppm), with the exception of the garnet-alkali-feldspar gneisses that show very low F contents, mostly below the detection limit of 20 ppm. Chlorine concentrations are mostly <200 ppm and similar in all rock types (a few samples contain up to 720 ppm). The notable exception is the two calc-silicate rock samples showing Cl contents of 825 and 2330 ppm.

In a similar way to Rb and Cs, the behaviour of Li and Sn can be related to their relative abundance in biotite and feldspars. Li contents are one order of magnitude higher in biotite (several hundred of ppm; Heier and Billings, 1978) than in feldspar (several tens of ppm; Smith, 1974; Smith and Brown, 1988). The same holds for Sn contents that are mostly <10 ppm in feldspar of igneous rocks, but at least ten times higher in biotite (e.g. Smith, 1974;

Hamaguchi and Kuroda, 1978). Therefore, the breakdown of biotite under granulite-facies conditions induces the partitioning of these elements into the fluid or melt phase and their depletion in the granulite-facies rocks due to partition coefficients between feldspars and silicic melts close to 1 for Li and significantly <1 for Sn (Larsen, 1979; Bea et al., 1994). Lastly, the breakdown of OH-bearing minerals (i.e. biotite) leads to the preferential partitioning of F into the melt phase and of Cl into the fluid phase (Carroll and Webster, 1994).

As a rule, depletion of U, Rb, Cs, Li, Sn, F and Cl in granulite-facies rocks implies removal of the fluid phase or of the melt phase (depending on the process leading to the breakdown of hydroxyl-bearing minerals) to prevent feed back-reactions. Therefore, granulite-facies metamorphism of crustal material appears as an efficient process for the mobilisation of a series of LIL and rare metals such as Sn, Li, Cs, and U, as well as help transfer them to upper crustal levels via a fluid or a melt phase.

3. Evidence of lithophile element traps

Well-characterized examples of trace elements liberated by granulite-facies metamorphism processes are relatively scarce. We will consider here the open system behaviour of some migmatitic domains, excluding geochemical exchanges between anatectic melts and their enclosing rocks during their injection or emplacement. Open-system behaviour during migmatisation has been invoked mainly for an external input of aqueous fluids (e.g. Mogk, 1992; Stevens, 1997; Brown, 2012). This is associated sometimes with the addition (Si, K) and/or removal (Ca) of major elements from the neosome (e.g. Hansen and Stuk, 1993), but rarely trace elements (Weber et al., 1985). The Tranomaro area in southern Madagascar, probably represent the most demonstrative example of fluid transfer from granulite-facies supracrustals to traps represented by skarns developed on a regional scale (Fig. 4; Moine et al., 1985). This example will be presented here first, followed by more limited data concerning the St Malo migmatites in the Armorican Massif, France (Weber et al., 1985) and migmatites from the Black Hills in South Dakota (Nabelek, 1999).

3.1. The Tranomaro pyroxenites

3.1.1. Regional geology

The Tranomaro area, southern Madagascar is composed of lower Proterozoic metasedimentary and metavolcanic rocks metamorphosed under granulite-facies conditions during the Pan-African orogeny, and belongs to the Mozambique mobile belt that extends into Sri Lanka and southern India (Paquette et al., 1994; Nicollet et al., 1995). The whole area is divided into three blocks by north-south, vertical, lithospheric-scale, shear zones (Pili et al., 1997a,b). The three blocks have undergone granulite-facies metamorphism (750–800 °C) with decreasing pressure from 1.1 GPa in the western block, to 0.8 GPa in the middle one and 0.4–0.5 GPa in the easternmost part of the Tranomaro block (Martelat et al., 1995, 1997). More specifically, the Tranomaro gneiss indicates low-pressure granulite-facies conditions (750–850 °C, 0.4–0.48 GPa) from qtz-pl-opx-grt assemblages (Rakotondrazafy et al., 1996) and high Xco_2 (0.82) in the fluid phase from qtz-bt-grt-sil-kfs assemblages (Ramambazafy et al., 1998). Th-U mineralization is found in the Tranomaro block (Rakotondratsima, 1983; Moine et al., 1985).

The Tranomaro gneiss comprises metapelites, commonly graphitic, abundant calc-silicate rocks and marbles, as well as siliceous gneiss; some of which correspond to former rhyolitic volcanic rocks (Fig. 4). The depositional environment of the sedimentary protoliths was typically a passive epicontinental

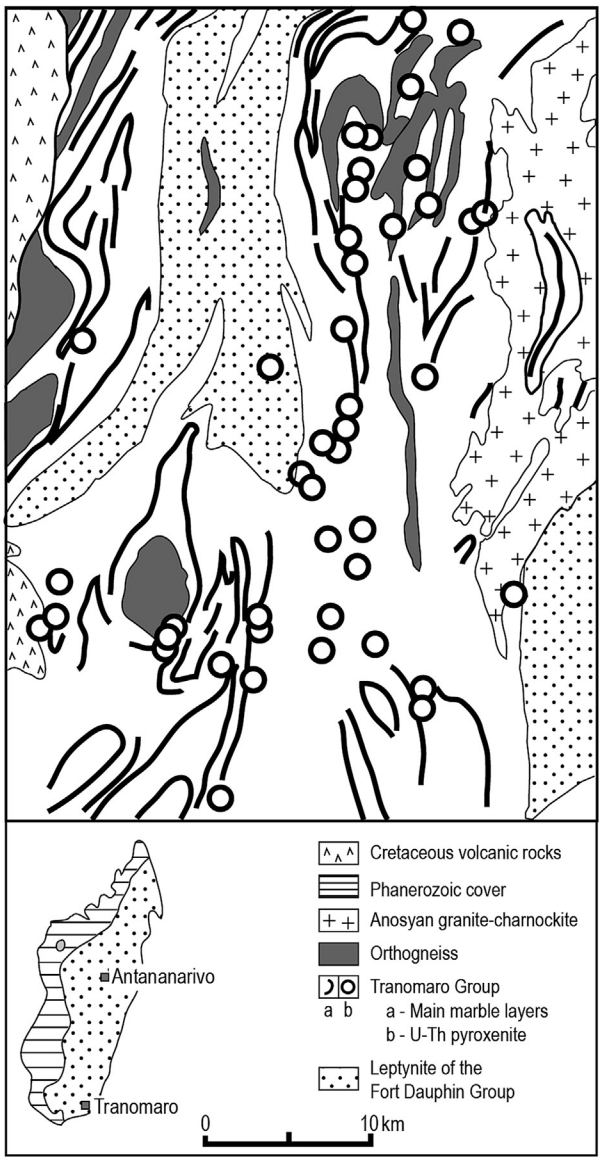

Figure 4. Simplified geological map of the Tranomaro area (modified after Boulvais et al., 1998). Only the largest granitic intrusions are represented. A map of Madagascar showing the location of the Tranomaro area is inserted.

margin setting. The marble layers are from a few metres up to a few hundred metres thick, and extend over several kilometres. Calc-silicate rocks are closely associated with marble. Some of them may have formed by metamorphism of impure limestone or marl, interlayered with the marble, producing polymineralic assemblages. Others have a metasomatic origin resulting from coupled element transfer between marble and granitic rocks or fluid injections, producing mostly monomineralic assemblages. The metasomatic calc-silicate rocks (hereafter referred to skarn) occur either as reaction zones between granite intrusions and host marble or as isolated layers at the contact with marble, with no evidence of a nearby granitic intrusion. Granite intrusions are generally small-sized and derived from the dehydration melting of biotite-bearing gneiss at depth, as described in the western deeper level blocks (Nicollet, 1985; Kröner et al., 1996).

Metasomatic skarns are generally well zoned, with the following successions that may extend over several metres to several tens of metres:

- biotite ± hypersthene granite;
- diopsidic syenite, the protolith being the granite from which quartz has been dissolved with silica having diffused into the enclosing marble, and Ca has migrated toward the granite to form diopside from biotite or hypersthene;
- scapolitite, essentially composed of the meionite end-member, with subordinate diopside, typically corresponding to an endoskarn;
- pyroxenite, essentially composed of pure Ca or Ca-Mg diopside, ± F-rich phlogopite ± scapolite, which corresponds to an exoskarn;
- marble, which may be composed only of carbonates or may have a complex mineralogy with forsterite ± F-rich phlogopite ± diopside ± dark green to light-coloured spinel ± F-rich humite ± wollastonite ± pargasite, depending on the amount of detrital Al-bearing silicates in the protolith. K-feldspar is sometimes present as small intergranular lenses; neither garnet nor graphite is present in the marble. Forsterite-bearing marble generally has a MgO content higher than 12 wt.%, whereas most diopside marble has a MgO content lower than 5 wt.%.

Granite is not always observed in the metasomatic zoning. For example in the Marosohy skarn occurrence the nearly mono-mineralic pyroxenite with some spinel and residual calcite is in sharp contact with a calcite-dolomite-forsterite-spinel marble (Boulvais et al., 2000). The amount of dolomite diminishes in the marble towards the pyroxenite with a relative increase in calcite and forsterite without the appearance of a new mineral phase. At the contact, diopside forms as forsterite disappears. The mineralogical zoning results from successive reactions induced by the infiltration of a silica-rich fluid and the subsequent production of CO_2.

Under retrograde conditions, F-rich phlogopite is associated with calcite, diopside, and occasional anhydrite, and forms veins crosscutting pyroxenite. Late-stage REE- and zircon-rich calcitic veins crosscut the calc-silicate complex.

3.1.2. Th-U mineralization

Numerous Th-U mineralized occurrences are known over several tens of kilometres in metasomatic skarns from the Tranomaro area (Fig. 4; Moreau, 1963; Moine et al., 1985). The main ore mineral is uranothorianite, which occurs as disseminated euhedral crystals, predominantly in diopsidic pyroxenite. The pyroxenite is always the most mineralized layer. However the uranothorianite also occasionally occurs in meionitic scapolitite and in the neighbouring marble. Centimetre-scale uranothorianite crystals may also occur in the veins phlogopite.

3.1.3. Genetic model

Two main stages of metasomatism have been identified in the Tranomaro area (Rakotondrazafy et al., 1996). The first stage, which corresponds to the main stage of the Th-U mineralization, includes aluminous diopside-scapolite-meionite-titanite-spinel-wollastonite-corundum-uranothorianite that records P-T conditions of 0.5 GPa and 850 °C at 565 Ma (Andriamarofahatra et al., 1990). The second stage, which is of minor importance for the mineralization, comprises F-phlogopite, F-pargasite, uranothorianite, and REE-rich hibonite. This assemblage formed at 800 °C and 0.3 GPa at 545 Ma (Paquette et al., 1994). The similarity between the ages and the P-T conditions demonstrates the synchronicity between granulite-facies metamorphism and the fluid circulation responsible for the first stage metasomatism and Th-U mineralization. Fluid inclusions in minerals from gneisses and skarns are CO_2-rich (Ramambazafy et al., 1998). Primary inclusions in growth zones from euhedral corundum crystals have isochores that intersect the P-T field defined by geothermobarometry from silicate minerals, indicating that they are synchronous with the peak metamorphic conditions (Rakotondrazafy et al., 1996; Ramambazafy et al., 1998).

Carbon dioxide was not the only fluid involved in the metasomatic reactions. In the Tranomaro metasomatic zones, the hydroxyl sites of phlogopite, pargasite, humite, and apatite are nearly saturated with F, suggesting that fluoride complexes may have transported simultaneously Th, U, REE, and Zr; all of which appear to be mobile in the metasomatic zones, together with Si and Ca (Moine et al., 1997; Boulvais et al., 2000). In particular, most of the Th/U ratios from the mineralized rocks are between 2 and 3, close to the average crustal ratio, and thus with no strong difference in mobility between U and Th. Also, unmixed aqueous brines may have coexisted with the carbonic fluids, as shown by Touret (1996) for granulite terrains, but not yet identified in the Tranomaro.

The $\delta^{13}C$ values, near 0‰ for the Tranomaro marbles, are typical of marine carbonates and thus provide no evidence for massive streaming of mantle-derived fluids during granulite-facies metamorphism. Localized but strong fluid flow occurred in the metasomatic mineralized zones, but also without any contribution from a deep-seated carbon source as evidenced by the carbon isotopic compositions of infiltrated marble and pyroxenite (Boulvais et al., 1998). The oxygen isotope compositions of pyroxenite are consistent with a purely crustal origin for the metasomatic reactions, Th-U mineralization, and rock-buffered fluids for marble. In addition, Nd isotopic compositions of metasomatized marble are similar to those from metasedimentary rocks and granite intrusions, indicating that the source of REE is either within the marble or from the granites (Boulvais et al., 2000).

A possible source for U and Th could be via synsedimentary pre-concentrations of Th, U, Zr, and REE in marl. However, this is unlikely because these elements in the sediments are mainly hosted by detrital monazite (Th, U and REE) and zircon (Zr mainly) that occur in relatively coarse siliciclastic sediments as placers. Marl, even that with a significant detrital component, never has high levels of these elements.

Another possible source, based mainly on the association of U with Th, REE and Zr, and on the presence of carbonate rocks with pyroxenite, could be a metamorphosed carbonatite. For example, the Th-U mineralization in Phalaborwa (South Africa) is associated with carbonatite and pyroxenite. Uranothorianite is the main ore mineral (Eriksson, 1989). However, U and Th concentrations in carbonatite are much lower, reaching only 25 ppm U at Phalaborwa. Such an origin will not explain the zoning observed between the different lithologies. Moreover, carbonatite bodies have high Nb contents that are not observed in the Tranomaro pyroxenite and associated carbonate rocks. The carbon isotopic composition of the Tranomaro marble is typical of marine carbonate rocks. A further convergence with carbonatite may be suggested by the recent description of silicocarbonatitic melts associated with the crystallization of phlogopite and diopside in the nearby Ampandrandava area (Martin et al., 2013; Morteani et al., 2013). However, the authors show that these melts result from the local partial melting of the crust and they do not report any enrichment in U or Th. Consequently, the geological, geochemical, and isotopic data are consistent with a synmetamorphic origin for the Th-U-REE-Zr mineralization, although these elements, especially U, are not usually expected to be enriched in granulite-facies rocks (Barbey and Cuney, 1982). The classic metasomatic zonation observed between the granite intrusions and the marble, dominantly controlled by the metasomatic exchange of Ca and Si between the two lithologies, and the isotopic compositions of the metasomatic rocks, imply that the Th-U-REE-Zr mineralization was derived from metasomatic fluids exsolved from syn-metamorphic granitic

magmas injected into the Tranomaro metamorphic series or from fluids derived from devolatization reactions occurring at depth during granulite-facies metamorphism. However, most of the metasomatized zones are not associated with a granite intrusion and seem to result from metamorphic fluid infiltration. The simultaneous mobility of U, Th, REE, and Zr is probably due to the high F contents in the fluids as a result of biotite breakdown.

3.2. Namaqualand and south Malawi granulites

In Namaqualand, South Africa (Andreoli et al., 2006), south Malawi, and Tete, Mozambique (Andreoli, 1984; Andreoli and Hart, 1990; Andreoli et al., 2011), it has been shown that the crust has been enriched in radiogenic elements during granulite-facies metamorphism, and even more that the radiogenic heat generated by the radioelement enrichment may be the cause of the granulite-facies metamorphism. In comparison with our study, the work done on the Namaqualand and South Malawi occurrences concern essentially magmatic rocks and associated fluids enriched in radiogenic elements and other incompatible elements, injected into supracrustal sequences, and does not focus on metasedimentary granulites. The authors attribute a mantle origin for the magma and fluids responsible for radiogenic element enrichment, but no stable isotope data are provided to support such an origin. The most striking enrichment observed in the Namaqualand area concerns Th which can reach economic concentrations in association with the REE in the Steenkampskraal monazite veins. However, the Th/U ratios of most Th-enriched lithologies are very high (up to 24 in the granites and orthogneisses; up to 44 in some charnockitic dykes; 78 for the Steenkampskraal monazite veins; and 288 in a leucodiorite from the Koperberg Suite), indicating the fractionation of U relative to Th (considering that the average Th/U chondritic ratio is about 4).

3.3. The migmatites of St Malo

The St Malo migmatitic dome consists of regionally metamorphosed Al-rich greywackes displaying all the stages of a progressive migmatisation (Martin, 1979). They represent a rather unique example where it can be demonstrated that the anatectic melts are derived from the surrounding gneisses (Martin, 1979; Weber et al., 1985). The migmatitic core of the dome is characterized by a K-feldspar-cordierite paragenesis. The P-T conditions of partial melting have been estimated with a temperature of about 720 °C for a pressure of 0.3 to 0.4 GPa.

Assuming non modal batch melting, petrogenetic modelling shows that the chemical patterns for most elements results from an interaction between equilibrium partial melting, mixing between melts, and residual mineral phases like low soluble accessory minerals and biotite. Generally a good mass balance is obtained between the restite, mesosomes, or parental gneisses and leucosomes, which give straight lines in the binary diagrams indicating closed system behaviour (e.g. Th/Y in Fig. 5a), Interestingly, elements easily mobile in a fluid phase, such as U or Rb, show an anomalous enrichment in most leucosomes (Fig. 5b–d). Such behaviour indicates an external influx for these elements seemingly introduced through a fluid phase, derived from deeper levels within the continental crust, which has been dissolved in the anatectic melt, and probably increased the rate of partial melting. It would be interesting to analyse a wider range of LIL and rare metals to determine if such behaviour is systematic for all these elements.

Similar open system behaviour has been observed mainly for U, Rb (Fig. 6), and Ta in migmatites from the Black Hills of South Dakota (Nabelek, 1999). Strong U enrichment in the leucosomes by input of an external fluid phase is necessary to explain the very low average Th/U ratios of the leucosomes (0.6), compared to those of the mesosomes (3.2) and the melanosomes (3.0), which remain close to the average crust value of 3.8. Similarly, Ta enrichment in the leucosomes is indicated by their higher Ta/Nb ratios (0.4) compared to those of the mesosomes and melanosomes, both of which are 0.1, a value close to the average crustal ratio. Two leucosomes have Ta/Nb ratios of 1.5 and 1.8 similar to those from extremely fractionated Rare Metal Granites (RMG) (see Table 2), without showing any anomalous enrichment in TiO_2, i.e. Ti-oxides

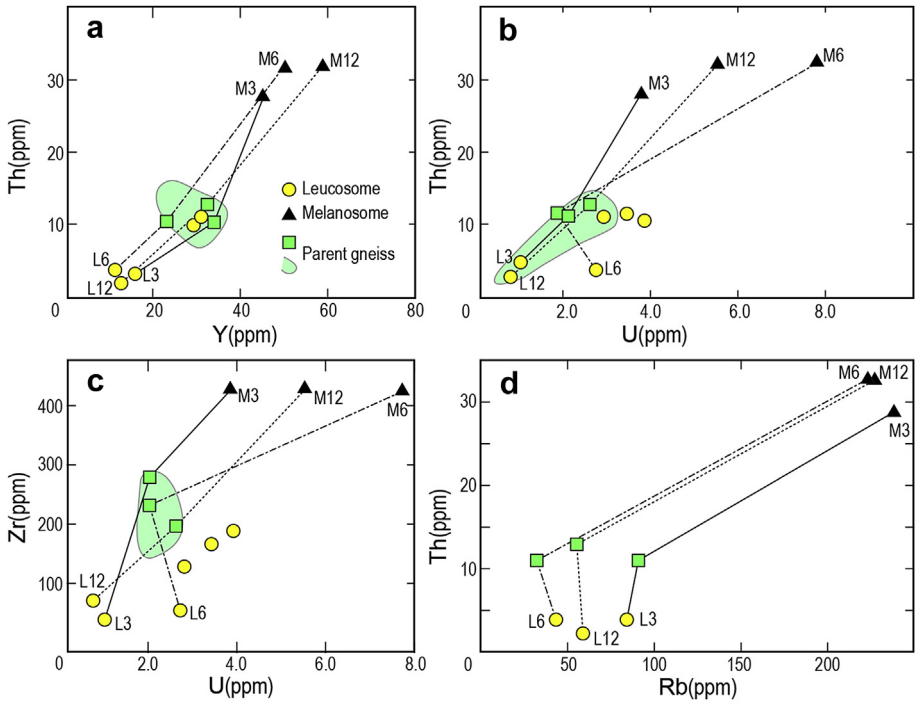

Figure 5. Fractionation of Y relatively to Th (a), of U relatively to Th (b) and Zr (c), and of Rb relatively to Th (d) in the St Malo migmatites. Data from Weber et al. (1985).

being known for their strong ability to incorporate Ta (Deer et al., 2013).

4. Granulite-facies metamorphism and Rare Metal Granites (RMG)

Most of the elements (e.g. Li, Rb, Cs, U, Sn, F), which are strongly depleted in granulite-facies metasedimentary rocks (e.g. the Lapland granulites), are particularly enriched in peraluminous high phosphorous (PHP) RMG and Pegmatites (Černý et al., 2005; Linnen and Cuney, 2008). The northern part of the French Massif Central provides a unique opportunity to examine the possible genetic link between late orogenic granulite-facies metamorphism of the lower continental crust and the genesis of a series of PHP-RMG intrusions (Cuney et al., 1992; Marignac and Cuney, 1999). In spite of the dominantly magmatic origin of rare-element granites, it is still difficult to explain their extreme degree of element enrichment and depletion by common magmatic processes (Linnen and Cuney, 2008).

4.1. Late Variscan orogenesis and granulite-facies metamorphism in the French Massif Central

The French Massif Central belongs to the western part of the mid-European Variscan belt. The Variscan orogeny can be divided into three geodynamic stages: the Eo-Variscan stage (Cambrian to Silurian), the Meso-Variscan stage (Devonian–early Carboniferous) and the Neo-Variscan stage (late Carboniferous–early Permian) (Matte, 2001).

During the Eo-Variscan stage, the northern part of Gondwana is fragmented and oceanic basins formed during the Cambrian to Ordovician period, which were then closed by subduction processes during the Silurian. The Meso-Variscan stage corresponds to the collision between the Gondwana and Baltica, with the formation of crustal-scale nappe structures and the intrusion of peraluminous granites. The Neo-Variscan stage is characterized by a shift from compressional to extensional tectonics during the late Stephanian and early Permian. It is noticeable that this stage is associated during the late Carboniferous (ca. 305 Ma; Costa et al., 1993), with the development of high heat flows, recorded by LP-HT metamorphism, extensive granite emplacement at middle to upper crustal levels, and granulite-facies metamorphism of the lower crust (Pin and Vielzeuf, 1983), as a result of the delamination of the lithospheric mantle (Pin, 1989; Costa and Rey, 1995).

Numerous hydrothermal deposits were formed during this last stage. These include W deposits at 325 and 310 Ma, RMG at about 310 Ma, shear-zone hosted Au and Sb deposits at about 300 Ma, and U deposits during the early Permian (270–280 Ma) (Marignac and Cuney, 1999).

4.2. Rare Metal Granite (RMG) emplacement

A series of RMG intrusions, strongly enriched in rare metal elements (Li, Rb, Cs, Sn, W, Ta, Nb, Be), were emplaced in the northern half of the French Massif Central (Fig. 7), within or in the vicinity of large peraluminous, two mica leucogranite complexes: Beauvoir (e.g., Aubert, 1969; Cuney et al., 1992; Raimbault et al., 1995); Montebras (Aubert, 1969); Blond (Burnol, 1974); Richemont (Raimbault and Burnol, 1998), La Chèze-Chédeville (Raimbault, 1998) and Chavence (Mourey, 1985). They have been nearly simultaneously emplaced around 310 ± 2 Ma, according to $^{40}Ar/^{39}Ar$ plateau ages obtained on Li-micas (Cheilletz et al., 1992; Cuney et al., 2002).

The shape of these intrusions, their emplacement level, and their spatial relations with associated peraluminous leucogranite complexes result in large variations. They range from pegmatites (Chédeville dykes, emplaced within the Saint-Sylvestre leucogranite complex), granites (Montebras laccolith, emplaced within the eastern Marche granite complex, or the Beauvoir cupola emplaced at the margin of the Colettes leucogranite), microgranites (the isolated Chavence cupola), to rhyolites (the Richemont rhyolite dike, emplaced in metamorphic rocks north of the Blond leucogranite) (Fig. 7).

4.3. Geochemical characteristics

All the RMG from the northern French Massif Central are extremely peraluminous (ASI = 1.42 to 1.53), particularly rich in Na (Na/K = 1.46 to 2.50), P (0.8 to 2.3 wt.% P_2O_5), and, with the exception of the Chavence microgranite, have relatively low SiO_2 contents (72.3 to 67.4 wt.% SiO_2) (Table 2). The geochemical characteristics discussed here are from the Beauvoir granite on which an extensive sampling is available thanks to existence of a 900 m deep bore hole (Cuney et al., 1992; Raimbault et al., 1995). The high Na and low silica contents of these granites result from the high F content of their parent magmas (0.85 to 2.43 wt.% F remaining presently in the crystallized granite), which shifted melt composition towards albite on the Q-Ab-Or triangle (Manning, 1981). Iron and Mn are present in moderate concentrations and are mainly hosted in the lepidolite-zinnwaldite solid solution, whereas Mg and Ti occur in very low concentrations. Due to the low solubility of zircon and monazite in such highly peraluminous, low-temperature melts (Watson and Harrison, 1983; Montel, 1993), the PHP-RMG are very poor in REE, Zr, Hf and Th (ppm to a few tens of ppm). In contrast, Rb, Cs, Li and Be are extremely enriched in

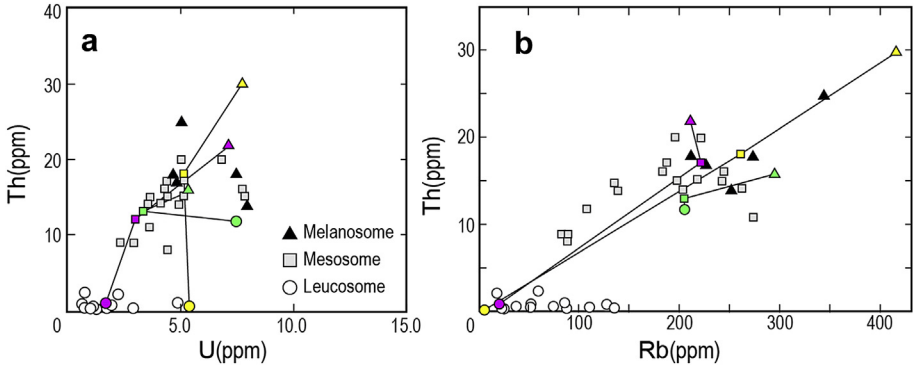

Figure 6. Fractionation of U relatively to Th (a) and Rb (b) in the Black Hills migmatites (South Dakota). Data from Nabelek (1999).

Table 2
Examples of composition of peraluminous high phosphorous granites from the French Massif Central and Portugal. Beauvoir (different units of the Beauvoir granite), Colettes and Montebras (Raimbault et al., 1995); Richemont (Raimbault and Burnol, 1998); Chédeville (Raimbault, 1998); and Argemela (Charoy and Noronha, 1996). LOI = Loss on ignition; n = number of samples; nd = no data; tr = traces.

	Beauvoir				Colettes	Montebras	Richemont	Chédeville	Argemela
	B1	B2	B3	B′2					
n	15	23	6	32	1	2	1	1	1
SiO_2	68.09	69.17	69.57	71.46	71.72	71.9	69.88	67.03	74.41
TiO_2	0.01	0.01	0.01	0.01	0.01	0.01	0.01	tr	tr
Al_2O_3	17.35	17.22	16.86	16.1	15.04	15.88	16.47	17.58	14.42
Fe_2O_3	0.15	0.25	0.44	0.51	1.13	0.25	0.02	0.19	tr
MnO	0.36	0.9	1.03	0.79	tr	0.65	0.11	0.17	0.05
MgO	0.22	0.37	0.4	0.26	0.12	0.52	0.02	tr	tr
CaO	0.45	0.5	0.82	0.39	0.58	1.84	1.21	0.19	0.01
Na_2O	4.94	4.63	4.39	4.49	3.28	3.92	3.43	3.95	2.55
K_2O	3.33	3.37	3.56	3.67	4.84	2.35	3.12	3.25	2.75
P_2O_5	1.46	1.73	1.75	1.06	0.43	1.49	1.17	0.98	2.16
L.O.I.	1.69	1.54	1.49	1.41	0.9	2.17	2.45	2.82	2.21
F (%)	2.51	2.22	1.67	1.66	nd	0.19	1.25	nd	0.53
								Range	
Li (ppm)	5762	3738	2201	2296	743	1205	3072	1800–6912	5532
Be	97	34	11	27	23	3	92.1	201–269	385
Cs	360	378	204	255	107	136	362	nd	350
Hf	2.6	2.1	1.9	1.2	29	3.6	2.59	1.06–1.93	4.7
Nb	91	49	39	49	601	95	85	43–130	46
Rb	3440	2478	1768	2013	82	1473	1933	1095–2166	2448
Sn	1175	961	590	347	14	1142	502	343–1077	746
Sr	126	150	274	92	10	69	97.7	16–358	<5
Ta	141	71	39	45	4.2	220	81.7	69–185	161
Th	0.65	0.48	0.38	0.42	20	0.9	0.31	0.86–2.41	0.9
U	11.3	15.9	18	14.9	38	6.4	14.2	2.7–11.5	15.4
W	22	30	19	54.6	47	17.5	5.9	8.2–27.1	5.9
Zr	28.3	20.2	26.3	26.8	9.4	12	13	21.0–32.5	13
La	0.77	0.65	0.79	1.37	24	0.248	0.145	0.16–2.36	0.145
Ce	1.24	1.46	1.01	0.87	1.41	2.66	0.434	0.36–4.21	4.1
A/NK	1.48	1.53	1.52	1.42	0.34	1.77	1.83	1.75	2.01
Ta/Nb	1.55	1.45	1.00	0.92		2.32	0.96	1.25–2.00	3.50

agreement with its fractionated character. Tungsten contents are high (up to 76 ppm), but not enriched at the same level as Ta or Sn, which reach very high concentrations, up to 425 and 1400 ppm respectively, in the most fractionated unit.

4.4. Genesis of Rare Metal Granites (RMG)

Most recent studies have shown that the unusual characteristics of the RMG granites and their rare metal concentration mainly

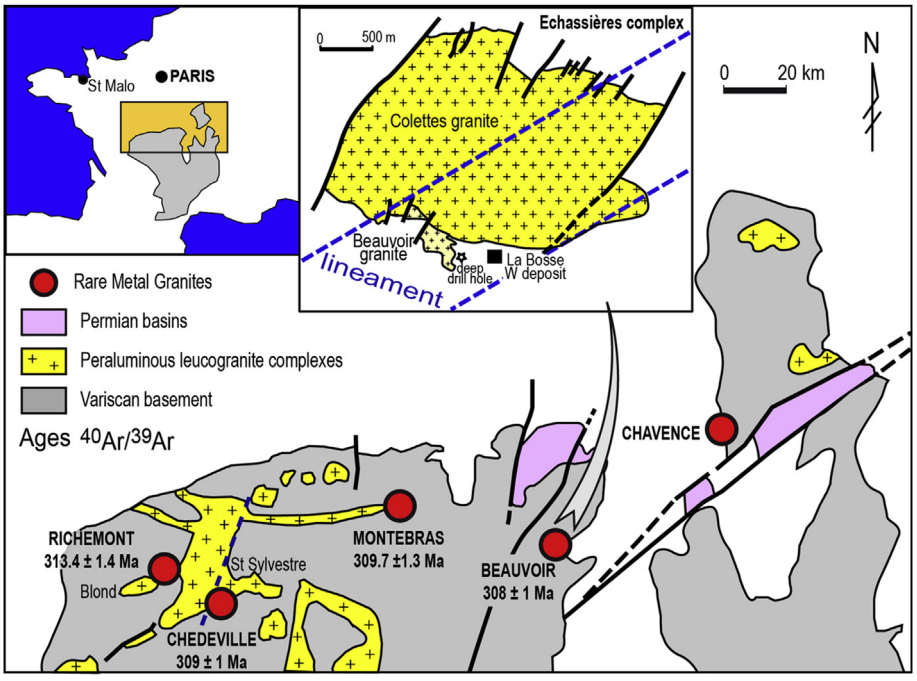

Figure 7. Distribution of the RMG relatively to the peraluminous leucogranitic complexes in the northern part of the French Massif Central (modified from Cheilletz et al., 1992). Permian basins from Héry (1990).

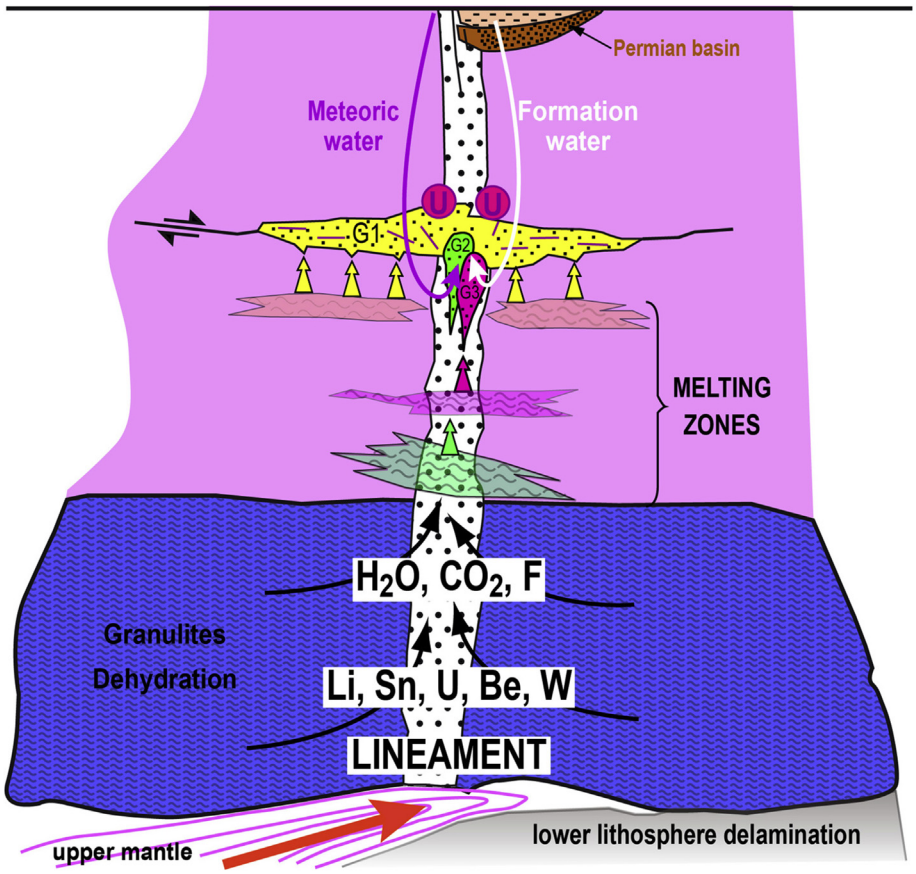

Figure 8. General model proposed for the genesis of RMG from partial melting of the crust induced by LIL and rare metal enriched fluids deriving from granulite-facies metamorphism during carbonic wave dehydration of underlying lower crust metasediments (modified from Cuney, 1990).

result from magmatic processes in a F-rich system, with a limited subsolidus redistribution of some elements (Pollard, 1989, 1995; Cuney et al., 1992; Raimbault et al., 1995; Černý et al., 2005; Linnen and Cuney, 2008). RMG are commonly interpreted as having resulted from the extreme fractionation of the larger peraluminous leucogranite complexes spatially associated with them (e.g., Černý, 1991; Linnen and Cuney, 2008). However, a series of data obtained on the RMG from the French Massif Central supports the hypothesis of an independent generation of RMG with respect to the associated large peraluminous leucogranite complexes (Cuney et al., 1992; Marignac and Cuney, 1999):

(1) The 3D geometry of the Beauvoir granite modelled from geological, structural, geochemical and geophysical data, shows that the feeding zone of the Beauvoir granite is not rooted in the Echassières granitic Complex, but orientated to the south of the Complex along the La Bosse lineament (Jacquot and Gagny, 1987), whereas the main roots of the Echassières granites are located in the middle of the complex (Vigneresse, 1987). Thus, these geometrical relations suggest that the feeding zone of the Beauvoir granite is independent from the Echassières granite.

(2) Many geochemical characteristics of the Beauvoir granite cannot be simply related through crystal fractionation to the spatially associated leucogranite complex (Table 2). For example the least fractionated Beauvoir granite, with about 72 wt.% SiO_2, has lower Fe_2O_3 content (0.7 wt.%) and much higher P content (0.8 wt.% P_2O_5) than the Colettes granite with the same silica content (1 wt.% Fe_2O_3, and only 0.4 wt.% P_2O_5). Similarly, weakly mobile elements at 72 wt.% SiO_2, such as Th and La, are more than ten times lower in the Beauvoir granite than in the Colettes granite (0.3 ppm vs. 4–5 ppm Th; 0.4 – 0.9 ppm vs. 9 ppm La), but three to ten times higher for Ta, Sn, Li, Rb, Cs in the Beauvoir granite compared to the Colettes granite (38 vs. 9–10 ppm Ta; 700 vs. 60 ppm Sn; 2500 vs. 600 ppm Li; 1800 vs. 550 ppm Rb; 300 vs. 110 ppm Cs) (Raimbault et al., 1995).

(3) Lastly, the most important evidence is the large time difference between the emplacement of all the RMG at 310 ± 2 Ma (Cheilletz et al., 1992; Cuney et al., 2002), irrespective of the age of the spatially associated leucogranite complexes, which are usually older. For example there is more than a 15 Ma time difference between the Chédeville pegmatites and associated Sagnes RMG granite cupola, and the St Sylvestre granite complex.

In addition to these features, it is remarkable that the generation of the RMG magmas from the northern part of the French Massif Central, was coeval with the extensive granulite-facies metamorphism of the lower crust in this area (ca. 310–290 Ma; Pin and Vielzeuf, 1983; Costa et al., 1993), induced by the delamination of the lower lithosphere. Cuney et al. (1994) proposed that fluids produced by the breakdown of micas were significantly enriched in LIL and rare metals and have induced a very low degree of partial melting in the intermediate crust, along deep-seated crustal structures ("lineaments") into which these fluids could have been channelled. For instance, the Beauvoir granite was emplaced along an N60°E lineament (Jacquot and Gagny, 1987). It is also remarkable that most of the W (±Sn) deposits at the scale of the French Massif Central also have a similar age at 310 ± 3 Ma for the northern part (Cuney et al., 2002).

The high concentrations of fluxing elements such as F, Li, P and sometimes B in these granitic melts strongly decrease their

viscosity and solidus temperature (London, 1987). Hence, these melts can be extracted from the source rocks at very low degrees of partial melting, and injected along narrow structures in upper crustal levels. Crystal-melt separation is also facilitated and protracted crystal-melt fractionation becomes possible, leading to the extreme LIL and rare-metal enrichment observed in the RMG magmas.

4.5. Other examples

In the succession of U enrichment processes which led to the formation of U deposits in the north-west French Massif Central, the emplacement of late intrusions enriched in U, F and, to a lesser extent, rare metals compared to the RMG (Fanay- and Sagnes-type fine-grained endogranitic intrusions) have a strong control on the genesis of U deposits (Cuney et al., 1989; Cuney, 1990). The Fanay-type intrusions are by far the most extensive and the most important for the control of the U deposits. Several features indicate that the Fanay granites are deriving from partial melting of the crust at deeper levels than the enclosing coarse-grained peraluminous leucogranites: (i) the Fanay granites are emplaced as a series vertical dykes, up to 2 km thick within a lineament zone where the enclosing granite exhibits vertical magmatic structures, instead of dominantly horizontal structures in the remaining part of the granitic complex and where gravimetric modelling indicates the deepest roots; (ii) the biotites of the Fanay granites are much richer in Ti (up to 4 wt.% TiO_2 in the Fanay granite instead of less than 1.5 wt.% in the enclosing granite) and F (up to 6 wt.% F in the Fanay granites instead of less than 1.8 wt.% F in the enclosing granite) (Monier, 1987); (iii) the modal amounts of zircon and monazite in these Fanay-type granites are also much higher as indicated by their distinct enrichment in Th, U, Zr, and REE (Friedrich et al., 1987; Cuney et al., 1989). The two last features are interpreted as reflecting the higher temperature involved in their genesis.

From these data, the anomalous enrichment in U, F and rare metals from the Fanay and Sagnes intrusions relative to the enclosing coarse-grained leucogranites has been interpreted as resulting from the enrichment of the magmas formed by partial melting in the middle crust by in U-, F- and rare metal-rich fluids deriving from the granulite-facies metamorphism of the lower crust in relation with the delamination of lower the lithosphere (Fig. 8) (Cuney, 1990; Marignac and Cuney, 1999). The same model is also proposed for the genesis of RMG occurring in the same part of the French Massif Central. The U deposits resulted from the leaching of U from the granites in the crustal shear zone by meteoric fluids, and their deposition by reduction thanks to a reduced fluid derived from an overlying Permian Basin. For more detailed explanations on the deposition of U as an ore, see Cuney (1990).

Two other examples from Portugal and Russia may also reflect the influence of fluids derived from granulite-facies metamorphism processes, but the evidence for either granite is less straightforward. The Argemela rare-element microgranite in Central Portugal (Charoy and Noronha, 1996) is interpreted as having resulted first from the injection of a quartz-albite-phengite crystal mush that was overprinted by a Li-F-P- and rare-element-rich phase. It is not clear whether the rare element-rich phase crystallized from a melt or a fluid-melt derived from melt immiscibility at deeper levels. It may also have originated from deeper levels of the continental crust during granulite-facies metamorphism.

A similar two stage enrichment process was also proposed by Reyf et al. (2000) and Badanina et al. (2004) to explain the extreme rare-element enrichment in the Orlovka RMG from the Khangilai complex in Transbaikalia, Russia. These authors proposed that the upper part of the pluton, the most Ta-enriched, resulted from the injection of an interstitial residual melt from deeper parts of the magmatic body into a previously solidified crystalline carapace at the top of the pluton.

5. Discussion and conclusions

5.1. Large ion lithophile (LIL) elements and rare metal flux from granulitized domains

The main mineralogical reaction leading to the granulite facies and the liberation of LIL and rare metals is the breakdown of biotite to anhydrous minerals such as K-feldspar plus cordierite, garnet or orthopyroxene, depending on the protolith composition, pressure, and temperature. The breakdown of biotite is essential since it is the host for most LIL (Rb, Cs, Li), F, Cl, and rare metals (Sn, W) (Neves, 1997), which are not incorporated in significant amounts into the newly formed anhydrous mineral paragenesis. Therefore, these elements strongly partition into the Cl- and F-rich fluids (or melt) resulting from granulite-facies phase transformations. Metasediments, especially metashales which commonly contain 30–50 vol.% mica at the onset of partial melting, and fractionated meta-granitic rocks are probably the best candidates to account for the liberation of large amounts of LIL, U, and rare metals, because they represent lithologies that are susceptible to be initially the most enriched in these elements.

Two main mechanisms can be invoked for the liberation of trace elements and rare metals during granulite-facies metamorphism, i.e. partial melting and carbonic wave dehydration. For the anatectic melts to be significantly enriched in these elements, a very low degree of partial melting would be required, probably in association with a protolith containing particularly high concentrations in these elements. The very low viscosity of such melts, highly enriched in F and Li (Holtz et al., 1993; Dingwell et al., 1996), may have facilitated their extraction from the source rocks even at a very low degree of partial melting (Baker and Vaillencourt, 1995). However, these melts, generated under granulite-facies conditions, should be characterized by high temperatures, which should have favoured an elevated solubility for the accessory minerals. Consequently, the less fractionated units of PHP-RMG, such as the B3 or B′2 unit of the Beauvoir granite, should show elevated concentrations in Th, REE and Zr, a characteristic that is actually not observed (Table 2). This mechanism may have operated for the PLP-RMG, which are more than one order of magnitude enriched in these elements (Linnen and Cuney, 2008). Moreover, as suggested by Rudnick and Presper (1990) from chemical modelling, the depletion in LIL in granulite-facies rocks is not easily accounted for by partial melting only, unless the entire melt fraction has been removed.

Even if partial melting, followed by protracted fractional crystallization, may represent a possible mechanism for the genesis of some RMG, the dehydration of the granulites by a carbonic wave appear to be a much more efficient process for the followings reasons: (i) the H_2O-bearing fluids, which are produced, are likely extremely enriched in F and Cl, two elements that are very efficient complexing anions for the transportation of rare metals; (ii) large quantities of LIL and rare metals can be liberated from the typically large volumes of lower crustal rock being subjected to dehydration; (iii) such fluids can easily be collected along the roots of trans-crustal scale shear zones; (iv) these fluids can be trapped in the middle crust where incipient partial melting may operate at lower temperatures and pressures as a function of the protolith chemistry or a decrease in the CO_2 partial pressure in the metamorphic fluid due to H_2O-CO_2 unmixing (e.g. Heinrich, 2007). This is especially efficient when the aqueous fluid has a high salinity (e.g. Touret and Huizenga, 2011); and (v) owing to the high F content in the

metamorphic fluids, more H_2O can dissolve in the melt (Holtz et al., 1993) enhancing the solubility of LIL and rare metals.

However, the model of a pervasive carbonic wave is still under debate. The fluid regime during granulite-facies metamorphism seems to be extremely variable from one place to another. Some workers have proposed that high-grade metamorphism is fluid-absent (Hoernes et al., 1994). Others have proposed that there is no significant C-O-H fluid flux across lithological contacts during high-grade metamorphism, but internal buffering of fluid activities by pore-fluids (Todd and Evans, 1993). Still others have suggested that the isotopic signatures are essentially pre-metamorphic with no evidence of pervasive fluid flow by mantle derived carbonic fluids (Boulvais et al., 1998). For example, oxygen and carbon isotopic data on the Rauer Group in East Antarctica (Buick et al., 1994) suggest a heterogeneous fluid regime, with no pervasive fluid flow in some localities, whereas other localities show evidence of fluid percolation predating high-grade metamorphism. Moreover, measurements of $\delta^{13}C$ in graphite from arrested charnockites are indicative of infiltration by a carbonic fluid via strong channelling (Santosh and Wada, 1993). Studies on large crustal-scale (up to 25 km wide) shear zones (Pili et al., 1997a,b) show evidence of percolation from mantle-derived carbonic fluids limited to the shear zones. The rocks outside the shear zones preserve the isotopic signatures of their protoliths. The non systematic origin of granulites by carbonic fluid percolation and the focussing of carbonic fluid percolation within the shear zones, which can reach a width of 25 km, may explain the relative scarcity of granitoids or pegmatites highly enriched in LIL and rare metals as well as their association with crustal scale shear zones such as the mineralized Tranomaro calc-silicate rocks, the Beauvoir rare metal granite, and the Fanay fine-grained granites from the Saint Sylvestre peraluminous leucogranite complex.

5.2. Consequences for ore deposit genesis

The depletion in LIL and rare metals, occurring during granulite-facies metamorphism, represents a powerful mechanism, which potentially could contribute to the genesis of several types of ore deposits in a manner more important than previously thought. The Tranomaro calc-silicate rocks represent a case of extreme metal enrichment (U, Th, REE, Zr) from metamorphic fluids and, to a lesser extent, from associated granitic melts, with limited fluid/melt migration. This enrichment occurred at very high temperatures and very high F activities. This allowed for the migration of very low soluble elements (Th, Zr, REE) together with U, within the granulite-facies domain itself, due to the presence of marble layers, which formed an efficient trap. Uranium and Rb enrichment in the St Malo migmatites (South Brittany, France) and U and Ta enrichment in the Black Hills migmatites (South Dakota) both occur at a higher structural level than in the Tranomaro calc-silicate rocks but with the observation of *in situ* enrichment within anatectic melts not extracted from their source. Such cases could well be more common, but geochemical analyses including LIL and rare metals are more the exception than the rule in the literature for such rocks. Anatectic pegmatites highly enriched in U-Th-REE are observed in migmatitic domains under P-T conditions close to that of granulite-facies. They may derive a part or all of their enrichment from such processes and not only from the partial melting of an U-Th-REE-rich protolith as is usually proposed (Cuney and Kyser, 2008; Mercadier et al., 2013).

Examples of more distal trapping, which has a more debatable connection to granulite-facies metamorphism, are seen in RMG from the northern French Massif Central, and in the fine-grained granites from the Saint Sylvestre peraluminous leucogranitic complex. The structural setting of these granites is a strong argument in favour of such a mechanism. The so called “lineaments” controlling their emplacement are interpreted as corresponding, at a higher structural level, to the same structures collecting metamorphic fluids from crustal domains experiencing granulite-facies metamorphism. Due to their high F and Li contents, these magmas have a relatively low viscosity, allowing rapid ascent along structures and associated efficient fractionation processes between already crystallized minerals and the silicate melts. The two stage enrichments described for some RMG intrusions (e.g., Argemela, Portugal and Orlovka, Russia), may also result from the infiltration of granulite derived LIL and rare metal loaded fluids, but this interpretation remains purely speculative at this stage.

5.3. Perspectives

This paper represents a first attempt to link the liberation of LIL and rare metals from lower crustal domains experiencing granulite-facies metamorphism with possible sinks for these elements at upper crustal levels. One of the major problems, which remains to be solved, concerns the partitioning of Ta and Nb into the fluid phase produced during the breakdown of the micas. Niobium and Ta are strongly partitioned into the pre-existing Ti-bearing minerals in the metamorphic protolith or produced by the breakdown of Ti-bearing minerals such as biotite, which have been segregated into the restitic phase. In the literature, reliable data on the behaviour of Ta and Nb under hydrothermal conditions did not exist until the recent experimental work of Zaraisky et al. (2010) and Korzhinskaya and Kotova (2012). Preliminary solubility data on Ta_2O_5, Nb_2O_5, natural columbite, and natural pyrochlore in 0.01 to 2 M HF and KF solutions at 550 °C and 1000 bar, under Co-CoO oxidizing conditions, show that acidic fluoride solutions with a high concentration of F are favourable for Nb and Ta solubility and transfer by aqueous fluids. Similar experiments should be developed at higher temperatures and in the presence of Ti-bearing minerals to verify if the partitioning coefficient for Nb and Ta is reduced in favour of columbite and pyrochlore and if their mobilization in an F-rich fluid phase is increased.

In order to further evaluate the fate of LIL and rare metal element transfer into metamorphic fluids and/or partial melts during granulite-facies metamorphism, and the transport of these fluids and melts into the upper crust, a wider data base concerning the concentration of these elements in migmatites located in the vicinity of granulite-facies terranes is needed. A more systematic analyses of these elements then needs to be undertaken.

Acknowledgement

This contribution is a tribute to Jacques Touret who was our professor at the University of Nancy. His enthusiasm for scientific research into fluids in the lower crust is largely responsible for our engagement in a career devoted to scientific research and more especially for our specific interest in deep crustal domains. The authors are grateful to Bernard Moine, Christian Marignac, Jacques Touret, Christian Pin, and Edward Sawyer, for fruitful discussions about the role of granulite facies metamorphism for trace element transfer. We would like to thank Philippe Boulvais and Marco Andreoli for their constructive reviews which help us to improve the manuscript. Daniel Harlov is thanked for his editorial supervision of the manuscript. This work was supported by the French National Research Agency through the national program “Investissements d’avenir” with the reference ANR-10-LABX-21 - RESSOURCES21.

References

Andreoli, M.A.G., 1984. Petrochemistry, tectonic evolution and metasomatic mineralisations of Mozambique Belt granulites from S. Malawi and Tete (Mozambique). Precambrian Research 25, 740–742.

Andreoli, M.A.G., Hart, R.J., 1990. Metasomatized granulites and eclogites of the Mozambique Belt: implications for mantle devolatilization. In: Herbert, H.K., Ho, E. (Eds.), Stable Isotopes and Fluid Processes in Mineralization. Geol Dept. and University Extension, the University of Western Australia, Publication 23, pp. 121–140.
Andreoli, M., Hart, R., Ashwal, L., Coetzee, H., 2006. Correlation between U, Th content and metamorphic grade in the western Namaqualand Belt, South Africa: with implications for radioactive heating of the crust. Journal of Petrology 47, 1095–1118.
Andreoli, M.A.G., Brandl, G., Coetzee, H., Kramers, J.D., Mouri, H., 2011. Intracrustal radioactivity as an important heat source for Neoarchaean metamorphism in the Central Zone of the Limpopo Complex. Geological Society of America Memoir 207, 143–161.
Andriamarofahatra, J., De La Boisse, H., Nicollet, C., 1990. Datation U-Pb sur monazites et zircons du dernier épisode tectonométamorphique granulitique majeur dans le Sud- Est de Madagascar. Comptes Rendus à l'Académie des Sciences 310, 1643–1648.
Aubert, G., 1969. Les coupoles granitiques de Montebras et d'Echassières (Massif Central Français) et la genèse de leur minéralisation en étain, tungstène, lithium et béryllium. Bureau de Recherche Géologiques et Minières, Mémoires 46, 234 p.
Badanina, E.V., Veksler, I.V., Thomas, R., Syritso, L.F., Trumbull, R.B., 2004. Magmatic evolution of Li-F, rare metal granites: a case study of melt inclusions in the Khangilay complex, Eastern Transbaikalia (Russia). Chemical Geology 210, 113–133.
Baker, D.R., Vaillencourt, J., 1995. The low viscosities of F + H_2O-bearing granitic melts and implications for melt extraction and transport. Earth and Planetary Science Letters 132, 199–211.
Barbey, P., Capdevila, R., Hameurt, J., 1982. Major and transition trace element abundances in the khondalite suite of the Granulite belt of Lapland (Fennoscandia). Evidence for an early Proterozoic flysch-belt. Precambrian Research 16, 273–290.
Barbey, P., Convert, J., Moreau, B., Capdevila, R., Hameurt, J., 1984. Petrogenesis and evolution of an early Proterozoic collisional orogenic belt: the Granulite belt of Lapland and the Belomorides (Fennoscandia). Bulletin of the Geological Society of Finland 56, 161–188.
Barbey, P., Cuney, M., 1982. K, Rb, Sr, Ba, U and Th geochemistry of the Lapland granulites (Fennoscandia). LILE fractionation controlling factors. Contributions to Mineralogy and Petrology 81, 304–316.
Barbey, P., Raith, M., 1990. The granulite belt of Lapland. In: Vielzeuf, D., Vidal, Ph. (Eds.), Granulites and Crustal Evolution, NATO ASI Series C. Kluwer, Dordrecht, pp. 111–132.
Bea, F., Pereira, M.D., Stroh, A., 1994. Mineral/leucosome trace-element partitioning in a peraluminous migmatite (a laser ablation-ICP-MS study). Chemical Geology 117, 291–312.
Bernard-Griffiths, J., Peucat, J.J., Postaire, B., Vidal, Ph., Convert, J., Moreau, B., 1984. Isotopic data (U-Pb, Rb-Sr, Pb-Pb and Sm-Nd) of mafic granulites from Finnish Lapland. Precambrian Research 23, 325–348.
Boulvais, P., Fourcade, S., Gruau, G., Moine, B., Cuney, M., 1998. Persistence of pre-metamorphic C and O isotopic signatures in marbles subject to Pan-African granulite-facies metamorphism and U–Th mineralization (Tranomaro. South-east Madagascar). Chemical Geology 150, 247–262.
Boulvais, P., Fourcade, S., Moine, B., Gruau, G., Cuney, M., 2000. Rare-earth elements distribution in granulite-facies marbles: a witness of fluid-rock interaction. Lithos 53, 117–126.
Brown, M., 2012. Open- and closed-system processes in the formation of migmatites and migmatitic granulites. Journal of Metamorphic Geology 30, 457–458.
Brown, G.C., Fyfe, W.S., 1970. The production of granitic melts during ultrametamorphism. Contributions to Mineralogy and Petrology 28, 310–318.
Buick, I.S., Harley, S.L., Cartwright, I., Mattey, D., 1994. Stable isotopic signatures of superposed fluid events in granulite facies marbles of the Rauer Group, East Antarctica. Journal of Metamorphic Geology 12 (3), 285–299.
Burnol, L., 1974. Géochimie du béryllium et types de concentration dans les leucogranites du massif central français. Bureau de Recherche Géologiques et Minières, Mémoires 85, 137 p.
Cagnard, F., Barbey, P., Gapais, D., 2011. Transition between "Archaean-type" and "modern-type" tectonics: Insights from the Finnish Lapland Granulite Belt. Precambrian Research 187, 127–142.
Carroll, M.R., Webster, J.D., 1994. Solubilities of sulfur, noble gases, nitrogen, chlorine, and flurorine in magmas. In: Carroll, M.R., Holloway, J.R. (Eds.), Volatiles in Magmas. Reviews in Mineralogy 30, 231–280.
Carron, J.P., Lagache, M., 1980. Etude expérimentale du fractionnement des éléments Rb, Cs, Sr et Ba entre feldspaths alcalins, solutions hydrothermales et liquides silicatés dans le système Q-Ab-Or-H2O à 2 kbar entre 700 et 800°C. Bulletin de Minéralogie 103, 571–578.
Černý, P., 1991. Fertile granites of Precambrian rare-element pegmatite fields: is geochemistry controlled by tectonic setting or source lithologies? Precambrian Research 51, 429–468.
Černý, P., Blevin, P.L., Cuney, M., London, D., 2005. Granite-related ore deposits. Economic Geology 100, 337–370.
Charoy, B., Noronha, F., 1996. Multistage growth of a rare-element, volatile-rich microgranite at Argemela (Portugal). Journal of Petrology 37, 73–94.
Cheilletz, A., Archibald, D., Cuney, M., Charoy, B., 1992. Ages 40Ar/39Ar du leucogranite à topaze-lépidolite de Beauvoir et des pegmatites sodolithiques de Chédeville (Nord Massif Central, France). Signification pétrologique et géodynamique. Comptes Rendus de l'Académie des Sciences 315 (3), 329–336.
Clemens, J.D., 1990. The granulite-granite connexion. In: Vielzeuf, D., Vidal, Ph. (Eds.), Granulites and Crustal Evolution, NATO ASI Series C, vol. 311. Kluwer, Dordrecht, pp. 25–36.
Clemens, J.D., Vielzeuf, D., 1987. Constraints on melting and magma production in the crust. Earth and Planetary Science Letters 86, 287–306.
Collerson, K.D., 1975. Contrasted patterns of K/Rb distribution in Precambrian high grade metamorphic rocks from Central Australia. Journal of the Geological Society of Australia 22 (2), 145–158.
Costa, S., Rey, P., Todt, W., 1993. Late Carboniferous age of lower-crustal granulite-facies xenoliths in the eastern French Massif Central: implications for post-thickening crustal processes. Abstract supplement n°1 Terra Nova 5, 233.
Costa, S., Rey, P., 1995. Lower crustal rejuvenation and growth during post-thickening collapse: Insights from a crustal cross section through a Variscan metamorphic core complex. Geology 23 (10), 905–908.
Cuney, M., 1990. Contrôles magmatiques et structuraux sur la métallogenèse tardi-hercynienne de l'uranium. Chronique de la Recherche Minière 499, 9–17.
Cuney, M., Alexandrov, P., Le Carlier, C., Cheilletz, A., Raimbault, L., Ruffet, G., 2002. The Sn-W-Rare Metals mineral deposits of the Western Variscan chain in their orogenic setting: the case of the Limousin area (French Massif Central). In: Blundell, D., Neubauer, F., von Quadt, A. (Eds.), The Timing and Location of Major Ore Deposits in an Evolving Orogen. Geological Society London, Special Publications 206, pp. 213–228.
Cuney, M., Friedrich, M., Blumenfeld, P., Bourguignon, A., Boiron, M.C., Vigneresse, J.L., Poty, B., 1989. Metallogenesis in the French part of the Variscan orogen. Part I: U preconcentration in pre-Variscan and Variscan formations – a comparison with Sn, W and Au. Tectonophysics 177, 39–57.
Cuney, M., Kyser, T.K., 2008. Deposits related to partial melting. In: Cuney, M., Kyser, T.K. (Eds.), Recent and Not-so-recent Developments in Uranium Deposits and Implications for Exploration, Short Course Series, vol. 39. Mineralogical Association of Canada, Québec, pp. 79–95.
Cuney, M., Marignac, C., Weisbrod, A., 1992. The Beauvoir topaz-lepidolite albitic granite (Massif Central France). A highly specialized granite with disseminated Sn-Li-Ta-Nb-Be mineralization of magmatic origin. Economic Geology 87, 1766–1794.
Cuney, M., Stussi, J.M., Marignac, C., 1994. A geochemical comparison between west- and central-European granites: implications for the origin of rare metal mineralization. In: Seltmann, R., Kämpf, H., Möller, P. (Eds.), Metallogeny of Collisional Orogens, Czech Geological Survey, pp. 96–102.
Daly, J.S., Balagansky, V.V., Timmerman, M.J., Whitehouse, M.J., de Jong, K., Guise, P., Bogdanova, S., Gorbatschev, R., Bridgwater, D., 2001. Ion microprobe U–Pb zircon geochronology and isotopic evidence for a trans-crustal suture in the Lapland-Kola orogen, Northern Fennoscandian Shield. Precambrian Research 105, 289–314.
Deer, W.A., Howie, R.A., Zussman, J., 2013. An Introduction to the Rock Forming Minerals. Mineralogical Society, 505 p.
Dingwell, D.B., Hess, K.-U., Knoche, R., 1996. Granite and granitic pegmatite melts: volumes and viscosities. Transactions of the Royal Society of Edinburgh: Earth Sciences 87, 65–72.
Dostal, J., Capedri, S., 1978. Uranium in metamorphic rocks. Contributions to Mineralogy and Petrology 66, 409–414.
Elo, S., 2006. Modelling the gravity anomaly of the Lapland Granulite Belt together with the results from the Finnish reflection experiment. In: Kukkonen, I.T., Lahtinen, R. (Eds.), Finnish Reflection Experiment FIRE 2001–2005, Geological Survey of Finland Special Paper, vol. 43, pp. 241–246.
Eriksson, S.C., 1989. Phalaborwa: a saga of magmatism, metasomatism and miscibility. In: Bell, K. (Ed.), Carbonatites, Genesis and Evolution. Unwin Hyman, London, pp. 221–254.
Evensen, N.M., Hamilton, M.J., O'Nions, R.J., 1978. Rare-earth abundances in chondritic meteorites. Geochimica et Cosmochimica Acta 42, 1199–1212.
Friedrich, M., Cuney, M., Poty, B., 1987. Uranium geochemistry in peraluminous leucogranites. Uranium 3, 353–385.
Fyfe, W.S., 1973. The granulite facies, partial melting and the Archaean crust. Philosophical Transactions of the Royal Society of London: Earth Sciences 273, 457–461.
Gaál, G., Berthelsen, A., Gorbatschev, R., Kesola, R., Lehtonen, M.I., Marker, M., Raase, P., 1989. Structure and composition of the Precambrian crust along the POLAR Profile in the northern Baltic Shield. Tectonophysics 162, 1–25.
Govindaraju, K., Mevelle, G., 1987. Fully automated dissolution and separation methods for inductively coupled plasma atomic emission spectrometry rock analysis. Application to the determination of rare earth elements. Plenary lecture. Journal of Analytical Atomic Spectrometry 2 (6), 615–621.
Govindaraju, K., Montanari, R., 1978. Routine performance of a matrix-correction free X-ray fluorescence spectrometric method for rock analysis. X-Ray Spectrometry 7 (3), 148–151.
Gray, C.M., 1977. The geochemistry of Central Australian granulites in relation to the chemical and isotopic effects of granulite facies metamorphism. Contributions to Mineralogy and Petrology 65, 79–89.
Hamaguchi, H., Kuroda, R., 1978. Tin. In: Correns, C.W., Shaw, D.M., Turekian, K.K., Zemann, J. (Eds.), Handbook of Geochemistry. Springer Verlag, Berlin, Heidelberg, New-York, pp. 1–7. II/4, 50-D.
Hansen, E., Stuk, M., 1993. Orthopyroxene-bearing, mafic migmatites at Cone Peak, California: evidence for the formation of migmatitic granulites by anatexis in an open system. Journal of Metamorphic Geology 11, 291–307.

Hansen, E.C., Janardhan, A.S., Newton, R.C., Prame, W.K.B.N., Ravindra Kumar, G.R., 1987. Arrested charnockite formation in southern India and Sri Lanka. Contributions to Mineralogy and Petrology 96, 225–244.
Heier, K.S., 1973. Geochemistry of granulite facies rocks and problems of their origin. Philosophical Transactions of the Royal Society of London: Earth Sciences 273, 429–442.
Heier, K.S., Billings, G.K., 1978. Lithium. In: Correns, C.W., Shaw, D.M., Turekian, K.K., Zemann, J. (Eds.), Handbook of Geochemistry. Springer Verlag, Berlin, Heidelberg, New-York, pp. 1–4. II/1, 3-D.
Heinrich, W., 2007. Fluid immiscibility in metamorphic rocks. Review in Mineralogy and Geochemistry 65, 389–430.
Héry, B., 1990. Potentialités en uranium des bassins permiens en France. Chronique de la Recherche Miniére 499, 60–66.
Hoernes, S., Fiorentini, E., Hoffbauer, R., 1994. The role of fluids in granulite-facies metamorphism as deduced from oxygen and carbon isotopic compositions. Precambrian Research 66, 183–198.
Holtz, F., Dingwell, D.B., Behrens, H., 1993. Effect of F, B_2O_3 and P_2O_5 on the solubility of water in haplogranitic melts compared to natural silicate melts. Contributions to Mineralogy and Petrology 113, 492–501.
Hörmann, P.K., Raith, M., Raase, P., Ackermand, D., Seifert, F., 1980. The granulite complex of Finnish Lapland: petrology and metamorphic conditions in the Ivalojoki-Inarijärvi area. Bulletin of the Geological Survey of Finland 308, 1–100.
Jacquot, T., Gagny, C., 1987. Pétrologie structurale du granite de Beauvoir: données et interprétation à son niveau apical. In: Cuney, M., Autran, A. (Eds.), Echassières: le forage scientifique. Une clé pour la compréhension des mécanismes magmatiques et hydrothermaux associés aux granites à métaux rares. Géologie de la France 2–3, 57–62.
Jahn, B.M., Auvray, B., Blais, S., Capdevila, R., Cornichet, J., Vidal, F., Hameurt, J., 1980. Trace element geochemistry and petrogenesis of Finnish greenstone belts. Journal of Petrology 21 (2), 201–244.
Janardhan, A.S., Newton, R.C., Hansen, E.C., 1982. The transformation of amphibolite facies gneiss to charnockite in southern Karnataka and northern Tamil Nadu, India. Contributions to Mineralogy and Petrology 79, 130–149.
Korzhinskaya, V.S., Kotova, N.P., 2012. Experimental modeling of possibility of hydrothermal transferring niobium by fluoride. Vestnik Otdelenia nauk o Zemle RAN 4, NZ9001. http://dx.doi.org/10.2205/2012NZ_ASEMPG.
Kriegsman, L.M., 2001. Partial melting, partial melt extraction and partial back reaction in anatectic migmatites. Lithos 56 (1), 75–96.
Kriegsman, L.M., Hensen, B.J., 1998. Back reaction between restite and melt: implications for geothermobarometry and pressure-temperature paths. Geology 26, 1111–1114.
Kröner, A., Braun, I., Jaeckel, P., 1996. Zircon geochronology of anatectic melts and residues from a high-grade pelitic assemblage at Ihosy, southern Madagascar: evidence for Pan- African granulite metamorphism. Geological Magazine 133, 311–323.
Larsen, L.M., 1979. Distribution of REE and other trace elements between phenocrysts and peralkaline undersaturated magmas, exemplified by rocks from the Gardar igneous province, south Greenland. Lithos 12 (4), 303–315.
Le Breton, N., Thompson, A.B., 1988. Fluid-absent (dehydration) melting of biotite in metapelites in the early stages of crustal anatexis. Contributions to Mineralogy and Petrology 99, 226–237.
Linnen, R.L., Cuney, M., 2008. Granite-related rare-element deposits and experimental constraints on Ta-Nb-W-Sn-Zr-Hf mineralization. In: Linnen, R.L., Samson, I.M. (Eds.), Rare-Element Geochemistry and Mineral Deposits. Geological Association of Canada, Short Course Notes 17, pp. 45–67.
London, D., 1987. Internal differentiation of rare-element pegmatites: effects of boron, phosphorous, and fluorine. Geochimica et Cosmochimica Acta 51, 403–420.
Manning, D.A.C., 1981. The effect of fluorine on liquidus phase relationships in the system Qz-Ab-Or with excess water at 1 kb. Contributions to Mineralogy and Petrology 76, 206–215.
Marignac, C., Cuney, M., 1999. Ore deposits of the French Massif Central: insight into the metallogenesis of the Variscan collision belt. Mineralium Deposita 34, 472–504.
Marker, M., Henkel, H., Lee, M.K., 1990. Combined gravity and magnetic modelling of the Tanaelv and Lapland Granulite Belts, Polar Profile Northern Baltic Shield. In: Freeman, R., Giese, P., Mueller, S. (Eds.), The European Geotraverse: Integrative Studies. European Science Foundation, Strasbourg, pp. 67–76.
Martelat, J.E., Nicollet, C., Lardeaux, J.M., Vidal, G., Rakotondrazafy, R., 1997. Lithospheric tectonic structures developed under high-grade metamorphism in the southern part of Madagascar. Geodinamica Acta 10, 94–114.
Martelat, J.-E., Vidal, G., Lardeaux, J.-M., Nicollet, C., Rakotondrazafy, M., 1995. Images spatiales et tectoniques profondes des continents: l'exemple du Sud-ouest de Madagascar. Comptes Rendus de l'Académie des Sciences 321 (2), 325–332.
Martin, H., 1979. Geochemical behavior of major and trace elements during incongruent melting of biotite in the St Malo massif migmatites (Bretagne, France). Neues Jahrbuch für Mineralogie Monatshefte 10, 509–524.
Martin, R.F., Randrianandraisana, A., Boulvais, P., 2013. Ampandrandava and similar phlogopite deposits in southern Madagascar formed from a silicocarbonatitic melt of crustal origin. Journal of African Earth Science. http://dx.doi.org/10.1016/j.jafrearsci.2013.08.002.
Matte, P., 2001. The Variscan collage and orogeny (480 ± 290 Ma) and the tectonic definition of the Armorica microplate: a review. Terra Nova 13, 122–128.
Maxwell, J.A., 1968. Rock and Mineral Analysis. Chemical Analysis. Wiley Publisher, 27, 584 p.
Mercadier, J., Annesley, I.R., McKechnie, C.L., Bogdan, T.S., Creighton, S., 2013. Magmatic and metamorphic uraninite mineralization in the western margin of the Trans-Hudson Orogen (Saskatchewan, Canada): a uranium source for unconformity-related uranium deposits? Economic Geology 108, 1037–1065.
Meriläinen, K., 1976. The granulite complex and adjacent rocks in Lapland, northern Finland. Bulletin of the Geological Survey of Finland 281, 1–129.
Mogk, D.W., 1992. Ductile shearing and migmatization at mid-crustal level in an Archaean high-grade gneiss belt, northern Gallatin Range, Montana, USA. Journal of Metamorphic Geology 10, 427–438.
Moine, B., Rakotondratsima, C., Cuney, M., 1985. Les pyroxénites à uranothorianite du Sud-Est de Madagascar: conditions physico-chimiques de la métasomatose. Bulletin de Minéralogie 108, 325–340.
Moine, B., Rakotondrazafy, M., Ramambazafy, A., Rakotondratsima, C., Cuney, M., 1997. Controls on the urano-thorianite deposits in SE Madagascar. In: Cox, R., Ashwal, L.D. (Eds.), Proceedings of the International Symposium Field Workshop on Proterozoic Geology of Madagascar. Gondwana Research Group Miscellaneous Publication 5, pp. 55–56.
Monier, G., 1987. Cristallochimie des micas des leucogranites. Nouvelles données expérimentales et applications pétrologiques (Unpublished PhD thesis). Orléans University, 288 p.
Montel, J.-M., 1993. A model for monazite/melt equilibrium and application to the generation of granitic magmas. Chemical Geology 110, 127–146.
Moreau, M., 1963. Le gisement des minéralisations de thorianite à Madagascar. Annales Géologiques de Madagascar 33, 175–178.
Morteani, G., Kostitsyn, Y.A., Gilg, H.A., Preinfalk, C., Razakamanana, T., 2013. Geochemistry of phlogopite, diopside, calcite, anhydrite and apatite pegmatites and syenites of southern Madagascar: evidence for crustal silicocarbonatitic (CSC) melt formation in a Panafrican collisional tectonic setting. International Journal of Earth Sciences 102, 627–645.
Mourey, Y., 1985. Le leucogranite à topaze de Chavence. Un nouvel exemple de massif à Sn, W, Li dans le nord du Massif Central Français. Comptes Rendus de l'Académie des Sciences 300 (2), 951–954.
Nabelek, P.I., 1999. Trace element distribution among rock-forming minerals in Black Hills migmatites, South Dakota: a case for solid-state equilibrium. American Mineralogist 84, 1256–1269.
Nash, W.P., Crecraft, H.R., 1985. Partition coefficients for trace elements in silicic magmas. Geochimica et Cosmochimica Acta 49, 2309–2322.
Neves, L.J.P.F., 1997. Trace element content and partitioning between biotite and muscovite of granitic rocks: a study in the Viseu region (Central Portugal). European Journal of Mineralogy 9, 849–857.
Newton, R.C., Smith, J.V., Windley, B.F., 1980. Carbonic metamorphism, granulites and crustal growth. Nature 288, 45–50.
Nicollet, C., 1985. The banded cordierite and garnet-bearing gneisses from Ihosy: a thermobaric tracer in southern Madagascar. Precambrian Research 28, 175–185.
Nicollet, C., Montel, J.-M., Foret, S., Martelat, J.E., Lardeaux, J.-M., 1995. E probe monazite dating of the uplift of the Precambrian in the south of Madagascar. In: Terra Abstract, vol. 7. European Union of Geosciences 8, Strasbourg, p. 124.
Paquette, J.-L., Nédélec, A., Moine, B., Rakotondrazafy, M., 1994. U-Pb, single zircon Pb-evaporation, and Sm-Nd isotopic study of a granulite domain in SE Madagascar. Journal of Geology 102, 523–538.
Pichamuthu, C.S., 1960. Charnockite in the making. Nature 188, 135–136.
Pili, E., Ricard, Y., Lardeaux, J.-M., Sheppard, S.M.F., 1997a. Lithospheric shear zones and mantle-crust connections. Tectonophysics 280, 15–29.
Pili, E., Sheppard, S.M., Lardeaux, J.M., Martelat, J.E., Nicollet, C., 1997b. Fluid flow vs. scale of shear zones in the lower continental crust and the granulite paradox. Geology 25 (1), 15–18.
Pin, C., 1989. Essai sur la chronologie et l'évolution géodynamique de la chaîne hercynienne d'Europe (Thèse de doctorat). Université Blaise Pascal, Clermont-Ferrand, 470 p.
Pin, C., Vielzeuf, D., 1983. Granulites and related rocks in Variscan median Europe: a dualistic interpretation. Tectonophysics 93, 47–74.
Pollard, P.J., 1989. Geologic characteristics and genetic problems associated with the development of granites-hosted deposits of tantalum and niobium. In: Möller, P., Cerný, P., Saupé, F. (Eds.), Lanthanides, Tantalum and Niobium. Springer Verlag, Berlin, pp. 237–253.
Pollard, P.J., 1995. A special issue devoted to the geology of rare metal deposits; geology of rare metal deposits; an introduction and overview. Economic Geology 90 (3), 489–494.
Raimbault, L., 1998. Composition of complex lepidolite-type pegmatites and of constituent columbite-tantalite, Chèdeville, Massif Central, France: a subvolcanic equivalent of rare-metal granites. Canadian Mineralogist 36, 563–583.
Raimbault, L., Burnol, L., 1998. The Richemont rhyolite dyke (French Massif Central): a subvolcanic equivalent of rare metal granites. Canadian Mineralogist 36, 265–282.
Raimbault, L., Cuney, M., Azencott, C., Duthou, J.L., Joron, J.L., 1995. Geochemical evidence for a multistage magmatic genesis of Ta-Sn-Li mineralization in the granite at Beauvoir, French Massif Central. Economic Geology 90, 548–576.
Raith, M., Raase, P., Hörmann, P.K., 1982. The Precambrian of Finnish Lapland: evolution and regime of metamorphism. Geologische Rundschau 71, 230–244.
Raith, M., Srikantappa, C., Shamanjari, K.G., Spieering, B., 1990. The granulite terrane of the Nilgiri Hills (Southern India): characterization of high-grade metamorphism. In: Vielzeuf, D., Vidal, Ph. (Eds.), Granulites and Crustal Evolution, NATO ASI Series C, vol. 311. Kluwer, Dordrecht, pp. 339–365.

Rakotondratsima, C., 1983. Les pyroxénites à urano-thorianite du Sud-Est de Madagascar. Etude pétrographique. minéralogique et géochimique. Conséquences métallogéniques (Unpubl. thesis). Université Claude Bernard Lyon I, 226 p.

Rakotondrazafy, M.A.F., Moine, B., Cuney, M., 1996. Mode of formation of hibonite ($CaAl_{12}O_{19}$) within the U–Th skarns from the granulites of SE Madagascar. Contributions to Mineralogy and Petrology 123, 190–201.

Ramambazafy, A., Moine, B., Rakotondrazafy, M., Cuney, M., 1998. Signification des fluides carboniques dans les granulites et les skarns du Sud-Est de Madagascar. Comptes Rendus de l'Académie des Sciences 327 (2), 743–748.

Reyf, F.G., Seltmann, R., Zaraisky, G.P., 2000. The role of magmatic processes in the formation of banded Li, F-enriched granites from the Orlovka tantalum deposit, Transbaikalia, Russia: microthermometric evidence. Canadian Mineralogist 38, 915–936.

Rudnick, R.L., Presper, T., 1990. Geochemistry of intermediate/- to high-pressure granulites. In: Vielzeuf, D., Vidal, Ph. (Eds.), Granulites and Crustal Evolution, NATO ASI Series C, vol. 311. Kluwer, Dordrecht, pp. 523–550.

Santosh, M., Wada, H., 1993. A carbon isotope study of graphites from the Kerala Khondalite Belt, southern India: evidence for infiltration in granulites. Journal of Geology 101, 643–651.

Senior, A., Leake, B.E., 1978. Regional metasomatism and the geochemistry of the Dalradian metasediments of Connemara, Western Ireland. Journal of Petrology 19, 585–625.

Smith, J.V., 1974. Feldspar Minerals. Springer-Verlag, New York, 627 p.

Smith, J.V., Brown, W., 1988. Feldspar Minerals. Second revised and extended edition. In: 1. Crystal Structures, Physical, Chemical and Microtextural Properties. Springer-Verlag, New York, 828 p.

Stevens, G., 1997. Melting, carbonic fluids and water recycling in the deep crust: an example from the Limpopo belt, South Africa. Journal of Metamorphic Geology 15, 141–154.

Taylor, S.R., McLennan, S.M., 1985. The Continental Crust: its Composition and Evolution. Blackwell Scientific Publications, Oxford, 312 p.

Thompson, A.B., 1982. Dehydration melting of pelitic rocks and the generation of H_2O-undersaturated granitic liquids. American Journal of Science 282, 1567–1595.

Todd, C.S., Evans, B.W., 1993. Limited fluid-rock interaction at marble-gneiss contacts during Cretaceous granulite-facies metamorphism, Seward Peninsula, Alaska. Contributions to Mineralogy and Petrology 114 (1), 27–41.

Touret, J.L.R., 1970. Le faciès granulite, métamorphisme en milieu carbonique. Comptes Rendus de l'Académie des Sciences 271 (2), 2228–2231.

Touret, J.L.R., 1971. Le faciès granulite en Norvège méridionale. II. Les inclusions fluides. Lithos 4, 423–435.

Touret, J.L.R., 1996. LILE-depletion in granulites: myth or reality? In: Demaiffe, D. (Ed.), Petrology and Geochemistry of Magmatic Suites of Rocks in the Continental and Oceanic Crusts, a Volume Dedicated to Pr. J. Michot. Université Libre de Bruxelles, Royal Museum for Central Africa, Tervuren, pp. 53–72.

Touret, J.L.R., Hartel, T.H.D., 1990. Synmetamorphic fluid inclusions in granulites. In: Vielzeuf, D., Vidal, Ph. (Eds.), Granulites and Crustal Evolution, NATO ASI Series C, vol. 311. Kluwer, Dordrecht, pp. 397–417.

Touret, J.L.R., Huizenga, J.M., 2011. Fluids in granulites. Geological Society of America Memoirs 207, 25–37.

Touret, J.L.R., Nijland, T.G., 2013. Prograde, peak and retrograde metamorphic fluids and associated metasomatism in upper amphibolite to granulite facies transition zones. In: Harlow, D.E., Austrheim, H. (Eds.), Metasomatism and the Chemical Transformation of Rock. The Role of Fluids in Terrestrial and Extraterrrestrial Processes. Lecture Notes in Earth System Sciences 2013. Springer, pp. 415–469 (Chapter 11).

Tuisku, P., Huhma, H., 2006. Evolution of migmatitic granulite complexes: implications from Lapland Granulite Belt, part II: Isotopic dating. Bulletin of the Geological Society of Finland 78, 143–175.

van de Kamp, P.C., Leake, B.E., Senior, A., 1976. The petrography and geochemistry of some Californian arkoses with application to identifying gneisses of metasedimentary origin. Journal of Geology 84, 195–212.

Vernet, M., Marin, L., Boulmier, S., Lhomme, J., Demange, J.C., 1987. Dosage du fluor et du chlore dans les matériaux géologiques, y compris les échantillons peralumineux. Analusis 15 (9), 490–498.

Veizer, J., 1978. Strontium. In: Wedepohl, K.H. (Ed.), Handbook of Geochemistry. Springer Verlag, Berlin, Heidelberg, New-York. II/4, 38 K and L.

Vielzeuf, D., Clemens, J.D., Pin, C., Moinet, E., 1990. Granites, granulites, and crustal differentiation. In: Vielzeuf, D., Vidal, Ph. (Eds.), Granulites and Crustal Evolution, NATO ASI Series C, vol. 311. Kluwer, Dordrecht, pp. 59–85.

Vielzeuf, D., Holloway, J.R., 1988. Experimental determination of the fluid-absent melting relations in the pelitic system. Consequences for crustal differentiation. Contributions to Mineralogy and Petrology 98, 257–276.

Vigneresse, J.-L., 1987. Organisation tridimensionnelle du massif d'Echassières et bilan des mesures géophysiques de surface. Géologie de la France 2–3, 27–32.

Watson, E.B., Harrison, T.M., 1983. Zircon saturation revisited: temperature and composition effects in a variety of crustal magma types. Earth and Planetary Science Letters 64, 295–304.

Weber, C., Barbey, P., Cuney, M., Martin, H., 1985. Trace element behaviour during migmatization. Evidence for a complex melt-residuum-fluid interaction in the St. Malo migmatitic dome (France). Contributions to Mineralogy and Petrology 90, 52–62.

Zaraisky, G.P., Korzhinskaya, V., Kotova, N., 2010. Experimental studies of Ta_2O_5 and columbite–tantalite solubility in fluoride solutions from 300 to 550°C and 50 to 100 MPa. Journal of Mineralogy and Petrology 99, 287–300.